Thermodynamically consistent phase field theory of phase transformations with anisotropic interface energies and stresses

Valery I. Levitas and James A. Warren

Phys. Rev. B **92**, 144106 — Published 13 October 2015

DOI: 10.1103/PhysRevB.92.144106

Thermodynamically consistent phase field theory of phase transformations with anisotropic interface energies and stresses

Valery I. Levitas[a], James A. Warren[b]

[a] *Iowa State University, Departments of Aerospace Engineering, Mechanical Engineering, and Material Science and Engineering, Ames, Iowa 50011, USA, vlevitas@iastate.edu and*

[b] *Material Measurement Laboratory, National Institute of Standards and Technology, Gaithersburg, Maryland 20899, U.S.*

Abstract

The main focus of this paper is to introduce, in a thermodynamically consistent manner, an anisotropic interface energy into a phase field theory for phase transformations. Here we use a small strain formulation for simplicity, but we retain some geometric nonlinearities, which are necessary for introducing correct interface stresses. Previous theories have assumed the free energy density (i.e., gradient energy) is an anisotropic function of the gradient of the order parameters in the current (deformed) state, which yields a nonsymmetric Cauchy stress tensor. This violates two fundamental principles: the angular momentum equation and the principle of material objectivity. Here, it is justified that for a noncontradictory theory the gradient energy must be an isotropic function of the gradient of the order parameters in the *current* state, which also depends anisotropically on the direction of the gradient of the order parameters in the *reference* state. A complete system of thermodynamically consistent equations is presented. We find that the main contribution to the Ginzburg-Landau equation resulting from small strains arises from the anisotropy of the interface energy, which was neglected before. The explicit expression for the free energy is justified. An analytical solution for the nonequilibrium interface and critical nucleus has been found and a parametric study is performed for orientation dependence of the interface energy and width as well as the distribution of interface stresses.

I. INTRODUCTION

The phase field approach (PFA) is routinely utilized for the simulation of various first-order phase transformations (PTs), including martensitic PTs [1–8], melting [9–14], twinning [15, 16], and grain growth [17]. In PFA, the energy density of the system depends on the so-called order parameters η_i, $i = 1, 2, ..., n$, and their gradients, in addition to the strain tensor and temperature. In most cases the order parameters represent internal variables (the exceptions are components of the strain tensor for martensitic PTs, e.g., [3, 8]), which describe material instabilities during structural changes in a continuous way. The energy of the system for each strain tensor and temperature has multi-well structure, i.e., it has a multiple local minima separated by energy barriers. Each minimum corresponds to a separate phase or structural state. Gradients of the order parameters are localized at the interfaces between phases and penalize the interface energy. The evolution of the microstructure is described by the Ginzburg-Landau equations, which are obtained as linear relationships between $\dot{\eta}_i$ **and their conjugates, the thermodynamic forces** X_i, together with a complete set of equations of continuum thermomechanics. In contrast to the sharp-interface approach, the solution exhibits finite-width interfaces, within which order parameters smoothly between the values corresponding to the local energy minima. Unlike sharp interface approaches, all one has to do is solve the above system of equations, there is no need for computational efforts to track interfaces.

Since strain tensor is one of the thermodynamic parameters that governs a PT, the PFA is combined with the strict description of the deformation process, see, e.g., text book on continuum mechanics [18]. The motion of a material will be described by a continuous function $\boldsymbol{r} = \boldsymbol{r}(\boldsymbol{r}_0, t)$, where $\boldsymbol{r}_0$ and $\boldsymbol{r}$ are the positions of points in the reference (undeformed) Ω_0 and the actual (deformed) Ω states (configurations), respectively, and t is the time. In general, deformation may or may not cause PTs.

Recently, significant efforts have been devoted to introducing interface stresses in the PFA. Initially, liquid-liquid and liquid-solid interfaces were treated, for which interface stresses play a key role. For a liquid-liquid interface the interface stresses represent biaxial tension with a magnitude equal to the interface energy γ (Fig. 1a). Since, at the nano- and even micro-scales, interface stresses are important for solid-liquid and solid-solid interfaces, and have been broadly studied within sharp-interface approach [19–27] as well molecular dynamics [28, 29], the **interface stresses have been introduced** in PFA as well, see [11, 12, 14, 30] for melting and [31–35] for solid-solid PTs. Here we will follow the most advanced theories at small strains [33] and large strains [35], where a detailed literature review is presented with critical analysis of the previous approaches. As the sharp-interface counterpart, we will start with the Shuttleworth equation [20, 27] for the magnitude $\bar{\sigma}^S$ of the interface stress,

$$\bar{\sigma}^S = \gamma + \partial\gamma/\partial\varepsilon_s = \bar{\sigma}_{st} + \bar{\sigma}_e^S, \tag{1}$$

where ε_s is the interface strain and subscript st means the structural part of the interface stresses. The interface stress consists of two contributions: (a) what we called the structural part, $\bar{\sigma}_{st} = \gamma$, as for a liquid-liquid interface, and (b) the part $\bar{\sigma}_e^S$ due to elastic deformation of an interface. We use a bar above the symbol σ for these "stresses", because stresses in Eq.(1) are localized at the zero-width interface and have dimensions **of force** per unit interface length rather than area.

Using the PFA, it is significant that the elastic contribution to the surface stresses comes directly from the solution of the Ginzburg-Landau and elasticity equations for a PT problem without any additional conditions. [12, 14, 30]. These contributions appear due to a heterogeneous distribution of the transformation strain and elastic moduli across a finite-width interface. Even for a solid-melt interface, elastic stresses in PFA are much higher than those obtained by molecular dynamics [28, 29], which leads to contradictions with the experimental data on the size dependence of the melting temperature for Al nanoparticles [14, 30]. To remedy this discrepancy, additional relaxation equations for the elastic interface stresses are

suggested in [14, 30] to obtain correspondence with experiments. Thus, even for melting, when shear modulus tends to zero across an interface, introducing extra elastic interface stresses would be harmful. That is why our main hypothesis in [14, 30, 32–35] is that *elastic interface stresses are completely defined from the solution of the Ginzburg-Landau and mechanics equations for a PT problem*. Thus, the main problem reduces to introducing the structural contribution to the interface stresses σ_{st} (see Fig. 1 with $\bar{\sigma}_{st} = \gamma$), i.e., as for liquid-liquid or liquid-gas interfaces.

This problem has been solved in [33, 34, 36] for small strain approximation and in [35] for general large strain formulation, but for the case of isotropic interface energy and, consequently, isotropic gradient energy $\psi^{\nabla}(\boldsymbol{\nabla}\eta_i)$. It is important to note that in order to introduce interface stresses (i.e., physical phenomenon) that represent biaxial tension with a magnitude equal to the nonequilibrium interface energy, it is necessary to introduce some geometrically nonlinear features even when strains are infinitesimally small. In particular, the gradient of the order parameters, $\boldsymbol{\nabla}\eta_i$, should be evaluated with respect to the deformed configuration. The *goal* of the current paper is to *generalize PFA presented in [33] for anisotropic interface energy* $\gamma(\boldsymbol{k})$*, i.e., for anisotropic function* $\psi^{\nabla}(\boldsymbol{\nabla}\eta_i)$, where $\boldsymbol{k} := \boldsymbol{\nabla}\eta_i/|\boldsymbol{\nabla}\eta_i|$ is the unit normal to the interface. Anisotropy of the interface energy plays a very important part in the solidification and growth of dendrites. Anisotropy determines morphology and kinetics of crystal growth, and is important for crystal-crystal phase transformation, fracture, and grain growth as well.

An anisotropic interface energy has been treated in numerous publications [9, 10, 13, 37–43]. by considering an anisotropic function of $\boldsymbol{\nabla}\eta_i$ in the deformed state, i.e., $\psi^{\nabla}(\boldsymbol{\nabla}\eta_i)$. However, the anisotropic function $\psi^{\nabla}(\boldsymbol{\nabla}\eta_i)$ results in a nonsymmetric contribution to the true (Cauchy) stress $\boldsymbol{\nabla}\eta_i \otimes \frac{\partial \psi^{\nabla}}{\partial \boldsymbol{\nabla}\eta_i}$ [33, 35, 37]. As we will discuss in Section II this leads to a violation of the angular momentum balance, which requires symmetry of the true stress. It is also possible to show that the stress power of the nonsymmetric stress is not invariant under superposition of the rigid-body rotation, which violates the principle of material objectivity.

However, these basic contradictions have never been mentioned in the previous publications. We will justify that in order to non-contradictorily describe anisotropic interface energy, the gradient energy should be an *isotropic* function of the gradient of the order parameters in the deformed state, $\boldsymbol{\nabla}\eta_i$, and in addition should depend on the direction of the normal to the interface in the reference (undeformed) state, $\boldsymbol{k}_0 := \boldsymbol{\nabla}_0\eta_i/|\boldsymbol{\nabla}_0\eta_i|$. This is consistent with the description of the anisotropic energy of the sharp interface in the undeformed state, $\gamma(\boldsymbol{k}_0)$, for which crystal lattice symmetry group is known, rather than in the deformed state, $\gamma(\boldsymbol{k})$, for which lattice symmetry also depends of the deformation gradient $\boldsymbol{F}$. For such a formulation, the true stress remains symmetric.

We would like to mention that there are various generic steps in some equation derivations for anisotropic interface energy that are the same or similar to those in [33] for isotropic energy. They will be repeated as briefly as possible and we will refer to [33] for detail.

The paper is organized as follows. In Section 2 the main problem formulation is justified, namely that the gradient energy should assume the form in $\psi^{\nabla}(|\boldsymbol{\nabla}\eta|, \boldsymbol{k}_0)$ for a single order parameter and $\psi^{\nabla} = \psi^{\nabla}(\boldsymbol{\nabla}\eta_k \boldsymbol{\cdot} \boldsymbol{\nabla}\eta_j, \boldsymbol{k}_{0i})$ for multiple order parameters, see Eq.(4). A thermodynamic treatment is performed in Section 3, including the derivation of the general structure of the constitutive equations. The expression for the free energy that results in the desired structure for the interface stress tensor, including its symmetry, is specified in Section 4. An explicit expression for the Ginzburg-Landau equations is analyzed in detail in Section 5. Anisotropy of the gradient energy produces many extra terms in these equations. Surprisingly, all of them are of the first degree of smallness for small strains, while the next term (transformation work) is of the third degree of smallness in strains. A complete system of equations is summarized in Section 6. In Section 7 an analytical solution for the nonequilibrium interface propagating in an arbitrary direction $\boldsymbol{k}$ is presented, and the temperature and orientation dependence of the interface energy and width is determined. Explicit results for a specific model are obtained in Section 8. The orientation dependence of the distribution of the interface stresses for a critical nucleus is given in Section 9. Section 10 contains

concluding remarks.

We designate the contractions of tensors $\boldsymbol{A} = \{A_{ij}\}$ and $\boldsymbol{B} = \{B_{ji}\}$ over one and two indices as $\boldsymbol{A}\cdot\boldsymbol{B} = \{A_{ij}\, B_{jk}\}$ and $\boldsymbol{A}\!:\!\boldsymbol{B} = A_{ij}\, B_{ji}$, respectively. The subscripts s and a designate the symmetric and the skew-symmetric part of a second-rank tensor; subscripts e, t, and θ mean elastic, transformational, and thermal strains; $\boldsymbol{I}$ is the unit tensor; δ_{ij} is the Kronecker delta; parameters in the undeformed state will be designated with subscript 0 and in the deformed state will not have any subscript; in particular, $\boldsymbol{\nabla}$ and $\boldsymbol{\nabla}_0$ are the gradient operators in the deformed and undeformed states, respectively; and $\otimes$ designates a dyadic product and $:=$ is equal by definition.

II. PROBLEM FORMULATION

A. Drawbacks of existing approaches

Sharp-interface approach. There are two driving forces for interface motion: (a) the Eshelby driving force for the translational interface motion [44–47]

$$X_\Sigma = -\Delta G - 2\gamma\kappa_{av}, \tag{2}$$

and (b) the Herring torque [48] for interface reorientation

$$\boldsymbol{X}_k = -\frac{\partial\gamma}{\partial\boldsymbol{k}}. \tag{3}$$

Here ΔG is the jump in the Gibbs energy across the interface and κ_{av} is the averaged interface curvature. While in Eq.(3) anisotropy of γ is the key to the existence of X_Σ, we keep isotropic γ in Eq.(2) for simplicity because here it is sufficient for our descriptive purpose. Both X_Σ and $\boldsymbol{X}_k$ are so-called thermodynamic configurational forces [44–47], which do not contribute explicitly to the equations of mechanics, namely, linear momentum balance and angular momentum balance. They do not describe the motion of material points, rather they describe the motion of interfaces with respect to the material. The confusion is often related

to the fact that when one determines a thermodynamically equilibrium position of interfaces and their junctions, the conditions are applied so that the resultant force and torque (or their work) are zero, i.e., like in mechanics. However, this is mechanics of configurational forces, which is independent of the linear and angular momentum balances. This is in contrast to the interface stresses, which do contribute to the momentum balance equation.

Phase field approach. An anisotropic interface energy within PFA was broadly studied in numerous publications [9, 10, 13, 37–43], in which the gradient energy is an anisotropic function of $\boldsymbol{\nabla}\eta_i$ in the current (deformed) state, i.e., $\psi^{\nabla} = \psi^{\nabla}(\boldsymbol{\nabla}\eta_i)$. However, there is a *conceptual contradiction* with the main principles of continuum mechanics in all these theories. Thus, the anisotropic function $\psi^{\nabla}(\boldsymbol{\nabla}\eta_i)$ results in a generally nonsymmetric contribution to the true (Cauchy) stress $\boldsymbol{\sigma}$ (i.e., force per current unit area) $\boldsymbol{\nabla}\eta_i \otimes \frac{\partial \psi^{\nabla}}{\partial \boldsymbol{\nabla}\eta_i}$ [10, 33, 35, 37]. This, however, violates the angular momentum balance, which requires symmetry of the true stress (see any textbook on continuum mechanics, e.g., [18]). It is also easy to show that the nonsymmetric stress tensor $\boldsymbol{\sigma}$ produces stress power $\boldsymbol{\sigma}{:}\boldsymbol{\nabla}\boldsymbol{v}^t$, where $\boldsymbol{v}$ is the particle velocity, that is not invariant under superposition of the rigid-body rotation in the deformed state, i.e., it contradicts the principle of material objectivity. Each of these contradictions make such a theory inadmissible from the point of view of traditional continuum mechanics. This, however, was completely overlooked in the previous theories.

Micropolar theory. Note that nonsymmetric stress is routinely used in a more general micropolar theory with some microstructure [49, 50], which rotates with respect to a continuum with some angular velocity. In this theory some body couples, the couple stress tensor, and the rotational moment of inertia equilibrate the antisymmetric part of the stress in the angular momentum balance. However, apart from the unjustified complexity, there are two reasons why this theory is not applicable for our case. First, changing the angular momentum equation due to orientation-dependence of the energy (i.e., the counterpart of the Herring torque) in PFA contradicts our statement that the Herring torque does not contribute to the moment of the momentum balance. Indeed, the driving force to interface

rotation in the PFA due to anisotropy of the gradient energy also should not change the angular momentum balance, similar to the fact that the driving force for change in order parameters (i.e., interface translational motion) does not change the momentum equation. Both are configurational forces that cause translational and rotational interface motion with respect to the material but do not produce mechanical torque and force that contribute to the angular momentum balance and momentum equation. *That is why the true stress tensor in PFA cannot be non-symmetric due to anisotropy of the interface energy and* ψ^{∇} *cannot be an anisotropic function of* $\boldsymbol{\nabla}\eta_i$. Second, we are unable to identify any meaningful rotating microstructure within a nm-thick interface that is not present in a bulk.

Remark. Many finite strain theories for melting, martensitic PT, twinning, and fracture utilize gradient of the order parameter in the reference configuration [15, 31, 51–54] and include anisotropy of the interface energy. We do not consider such an approach here because it results in $\boldsymbol{\sigma}_{st} = 0$**.**

B. Problem formulation

Sharp-interface approach. An important question is: should γ depend on the unit normal $\boldsymbol{k}$ in the deformed state or on the unit normal $\boldsymbol{k}_0$ in the undeformed state? Since the symmetry group of the crystal lattice is well-defined in the undeformed state only, the interface energy γ can be presented as a function $\gamma(\boldsymbol{k}_0)$, which is invariant with respect to the symmetry group of the undeformed lattice. Since deformation of the lattice described by the deformation gradient $\boldsymbol{F}$ changes its symmetry, the interface energy cannot be a function of $\boldsymbol{k}$ only but must also depend on $\boldsymbol{F}$, i.e., $\gamma = \gamma(\boldsymbol{k}, \boldsymbol{F})$. The only way to determine this function is to find the $\gamma(\boldsymbol{k}_0)$ that corresponds to the symmetry of the undeformed lattice and express $\boldsymbol{k}_0$ in terms of $\boldsymbol{k}$ and $\boldsymbol{F}$. This is similar to the formulation of strain energy for an anisotropic elastic material: it is formulated in the undeformed state and, if desired, is expressed in terms of strain measures defined in the deformed state.

Phase field approach. Similar consideration will be applied here. For an isotropic interface energy the correct expression for the gradient energy that results in the desired expression for the interface stresses is $\psi^{\nabla}(|\boldsymbol{\nabla}\eta|)$ for a single order parameter and $\psi^{\nabla} = \psi^{\nabla}(\boldsymbol{\nabla}\eta_k \cdot \boldsymbol{\nabla}\eta_j)$ for the multiple order parameters. For a single order parameter and anisotropic interface energy, the options are $\psi^{\nabla}(|\boldsymbol{\nabla}\eta|, \boldsymbol{k}_0)$ or $\psi^{\nabla}(|\boldsymbol{\nabla}\eta|, \boldsymbol{k}) = \tilde{\psi}^{\nabla}(\boldsymbol{\nabla}\eta)$. The second option has already been explored [10, 33, 35, 37] and results in a nonsymmetric stress tensor, which, as we found, is forbidden. The first option, since the second argument, $\boldsymbol{k}_0$, is strain-independent it does not change the general expression for stress compared to the isotropic case, i.e., the stress tensor remains symmetric (see Section IV). The function $\psi^{\nabla}(|\boldsymbol{\nabla}\eta|, \boldsymbol{k}_0)$ also corresponds to $\gamma(\boldsymbol{k}_0)$ for a sharp interface and can be made invariant with respect to a known symmetry group of the undeformed crystal lattice. Similarly, for multiple order parameters, the anisotropy should be described in terms of $\boldsymbol{k}_{0i}$. Consequently, we will develop a theory below based on the symmetric stress tensor and gradient energy of the form

$$\psi^{\nabla} = \psi^{\nabla}(\boldsymbol{\nabla}\eta_k \cdot \boldsymbol{\nabla}\eta_j, \boldsymbol{k}_{0i}) \quad \text{or} \quad \psi^{\nabla}(|\boldsymbol{\nabla}\eta|, \boldsymbol{k}_0). \tag{4}$$

III. THERMODYNAMIC TREATMENT

Due to the necessity of distinguishing between deformed and undeformed states, allowing for anisotropy of the interface energy in PFA can be done strictly in the framework of fully large strain formulation only, i.e., by generalizing results obtained in [35]. This is what we did, **and then we simplified the *final* results for small strains to obtain consistent linearization.** However, to simplify the presentation and to broaden our audience, we started with a geometrically linear formulation and **kept only those geometrically nonlinear terms, which we found by simplifying the strict theory.**

Let small distortions of a material be described by a continuous function $\boldsymbol{r} = \boldsymbol{r}(\boldsymbol{r}_0, t)$, where $\boldsymbol{r}_0$ and $\boldsymbol{r}$ are the positions of points in the reference (undeformed) Ω_0 and the actual

(deformed) Ω states (configurations), respectively, and t is the time. Assume that at time t_0 the material is in the high symmetry phase H and it may be transformed into a number of lower symmetry phases L_i, which may include martensitic variants. Each of the PTs $\mathsf{H}\leftrightarrow\mathsf{L}_i$ are described by a corresponding order parameter η_i with $\eta_i = 0\ \forall i$ for H and $\eta_k = 1$, $\eta_i = 0$ $\forall i \neq k$ for L_k. The deformation gradient is $\boldsymbol{F} = \frac{\partial \boldsymbol{r}}{\partial \boldsymbol{r}_0} = \nabla_0 \boldsymbol{u} + \boldsymbol{I} \simeq \boldsymbol{I} + \boldsymbol{\varepsilon} + \boldsymbol{\omega}$, where $\boldsymbol{\varepsilon} = (\nabla_0 \boldsymbol{u})_s$ and $\boldsymbol{\omega} = (\nabla_0 \boldsymbol{u})_a$ are small in comparison with unity symmetric strain and antisymmetric rotation tensors, respectively, and $\boldsymbol{u}$ is the displacement vector. The inverse deformation gradient is $\boldsymbol{F}^{-1} \simeq \boldsymbol{I} - \boldsymbol{\varepsilon} - \boldsymbol{\omega}$, which is easy to check: $\boldsymbol{F} \cdot \boldsymbol{F}^{-1} = \boldsymbol{I} - \boldsymbol{\varepsilon}\cdot\boldsymbol{\varepsilon} - \boldsymbol{\omega}\cdot\boldsymbol{\omega} - \boldsymbol{\omega}\cdot\boldsymbol{\varepsilon} - \boldsymbol{\varepsilon}\cdot\boldsymbol{\omega} \simeq \boldsymbol{I}$. We employ an additive decomposition of the strain tensor $\boldsymbol{\varepsilon}$

$$\boldsymbol{\varepsilon} = \boldsymbol{\varepsilon}_e + \boldsymbol{\varepsilon}_t(\eta_i) + \boldsymbol{\varepsilon}_\theta(\theta, \eta_i) \tag{5}$$

into elastic $\boldsymbol{\varepsilon}_e$, transformational $\boldsymbol{\varepsilon}_t$, and thermal $\boldsymbol{\varepsilon}_\theta$ parts.

Since we retain a symmetric stress tensor we can repeat the same thermodynamic treatment as in [33] and we arrive at the following dissipative inequality (see Eq.(10) in [33]):

$$\rho_0\, \mathcal{D} \,=\, \boldsymbol{\sigma} : \dot{\boldsymbol{\varepsilon}} - \rho_0\, \dot{\psi} - \rho_0\, s\, \dot{\theta} \,+ \boldsymbol{\nabla}_0 \cdot (\boldsymbol{Q}_i^\eta \dot{\eta}_i) \,\geq\, 0\ . \tag{6}$$

Here, $\mathcal{D}$ is the rate of dissipation per unit mass, ρ_0 is the mass density per unit undeformed volume, ψ and s are the specific Helmholtz free energy and the entropy, both per unit mass, θ is the temperature, and $\boldsymbol{Q}_i^\eta$ are generalized forces conjugate to $\dot{\eta}_i$ at the surface of a sample, which are introduced in order to balance terms due to the dependence of the thermodynamic potential on $\boldsymbol{\nabla}_0 \eta_i$. While in [33] this equation was written in terms of parameters (mass densities and gradient operator) determined for the deformed state, it will be more straightforward to perform derivations for anisotropic gradient energy if we use parameters determined per unit undeformed state. Because of the small strain approximation, both approaches are equivalent, and we will change some parameters (e.g., ρ) from undeformed to deformed value for convenience without additional discussion.

Let $\psi = \psi(\boldsymbol{\varepsilon}, \eta_i, \theta, \boldsymbol{\nabla}_0 \eta_i, \boldsymbol{\nabla} \eta_i) = \psi(\boldsymbol{\varepsilon}, \eta_i, \theta, \boldsymbol{\nabla}_0 \eta_i, \boldsymbol{\nabla}_0 \eta_i \cdot \boldsymbol{F}^{-1}) = \psi(\boldsymbol{\varepsilon}, \eta_i, \theta, \boldsymbol{\nabla}_0 \eta_i, \boldsymbol{\nabla}_0 \eta_i \cdot (\boldsymbol{I} - \boldsymbol{\varepsilon} - \boldsymbol{\omega}))$, where we used $\boldsymbol{\nabla} \eta_i = \boldsymbol{\nabla}_0 \eta_i \cdot \boldsymbol{F}^{-1}$. Since ψ must be invariant with respect to the

superposed rigid-body rotation, it cannot depend on $\boldsymbol{\omega}$. Thus, the objective form of ψ is $\psi = \psi(\boldsymbol{\varepsilon}, \eta_i, \theta, \boldsymbol{\nabla}_0\eta_i, \boldsymbol{\nabla}_0\eta_i \cdot (\boldsymbol{I} - \boldsymbol{\varepsilon})) = \bar{\psi}(\boldsymbol{\varepsilon}, \eta_i, \theta, \boldsymbol{\nabla}_0\eta_i)$. We will also need $\boldsymbol{\nabla}_0 \cdot (\boldsymbol{Q}_i^\eta \dot{\eta}_i) = (\boldsymbol{\nabla}_0 \cdot \boldsymbol{Q}_i^\eta)\dot{\eta}_i + \boldsymbol{Q}_i^\eta \cdot \boldsymbol{\nabla}_0\dot{\eta}_i$. Substituting $\dot{\psi}$ and the above equation into Eq.(6), we obtain

$$\rho_0 \mathcal{D} = \left(\boldsymbol{\sigma} - \rho_0 \frac{\partial \bar{\psi}}{\partial \boldsymbol{\varepsilon}}\right) : \dot{\boldsymbol{\varepsilon}} - \rho_0 \left(s + \frac{\partial \bar{\psi}}{\partial \theta}\right) \dot{\theta} - \left(\rho_0 \frac{\partial \bar{\psi}}{\partial \eta_i} - \boldsymbol{\nabla}_0 \cdot \boldsymbol{Q}_i^\eta\right) \dot{\eta}_i + \left(\boldsymbol{Q}_i^\eta - \rho_0 \frac{\partial \bar{\psi}}{\partial \boldsymbol{\nabla}_0 \eta_i}\right) \cdot \boldsymbol{\nabla}_0 \dot{\eta}_i \geq 0. \tag{7}$$

The usual assumption that the dissipation rate is independent of $\dot{\theta}$ and $\boldsymbol{\nabla}_0\dot{\eta}_i$ leads to the constitutive equations for the entropy and generalized thermodynamic forces $\boldsymbol{Q}_i^\eta$:

$$s = -\frac{\partial \bar{\psi}}{\partial \theta}; \qquad \boldsymbol{Q}_i^\eta = \rho_0 \frac{\partial \bar{\psi}}{\partial \boldsymbol{\nabla} \eta_i}. \tag{8}$$

The residual dissipative inequality is

$$\rho_0 \mathcal{D} = \boldsymbol{\sigma}_d : \dot{\boldsymbol{\varepsilon}} + \rho_0 X_i \dot{\eta}_i \geq 0, \tag{9}$$

where the dissipative stress $\boldsymbol{\sigma}_d$ is equal to the parenthesis in front of $\dot{\boldsymbol{\varepsilon}}$ and the dissipative force X_i is equal to the parenthesis in front of $\dot{\eta}_i$. This results in constitutive equations for the stress tensor and an evolution equation for η_i

$$\boldsymbol{\sigma} = \rho_0 \frac{\partial \bar{\psi}}{\partial \boldsymbol{\varepsilon}} + \boldsymbol{\sigma}_d; \qquad X_i = -\frac{\partial \bar{\psi}}{\partial \eta_i} + \frac{1}{\rho_0} \boldsymbol{\nabla} \cdot \left(\rho_0 \frac{\partial \bar{\psi}}{\partial \boldsymbol{\nabla} \eta_i}\right), \tag{10}$$

assuming that constitutive equations for $\boldsymbol{\sigma}_d$ and X_i are given. For initially homogeneous material, which we will consider below, ρ_0 disappears from Eq.(10) for X_i. The assumption about thermodynamic independence of processes described by $\dot{\boldsymbol{\varepsilon}}$ and $\dot{\eta}_i$ leads to two separate inequalities, $\boldsymbol{\sigma}_d : \dot{\boldsymbol{\varepsilon}} \geq 0$ and $X_i \dot{\eta}_i \geq 0$. They can be satisfied if at least $\boldsymbol{\sigma}_d = \boldsymbol{\sigma}_d(\dot{\boldsymbol{\varepsilon}})$ and $X_i = X_i(\dot{\eta}_j)$.

IV. STRUCTURE OF THE HELMHOLTZ FREE ENERGY AND EXPRESSION FOR STRESSES

A. Structure of the Helmholtz free energy

The structure of the Helmholtz energy will be used similarly to that in [33]

$$\bar{\psi}(\boldsymbol{\varepsilon},\eta_i,\theta,\boldsymbol{\nabla}\eta_i,\boldsymbol{\nabla}_0\eta_i)=\frac{J_{t\theta}}{\rho_0}\psi^e(\underbrace{\boldsymbol{\varepsilon}-\boldsymbol{\varepsilon}_t(\eta_i)-\boldsymbol{\varepsilon}_\theta(\theta,\eta_i)}_{\boldsymbol{\varepsilon}_e},\eta_i,\theta)+J\breve{\psi}^\theta(\theta,\eta_i)+\tilde{\psi}^\theta(\theta,\eta_i)+$$
$$J\psi^\nabla(\boldsymbol{\nabla}\eta_k\cdot\boldsymbol{\nabla}\eta_j,\boldsymbol{k}_{0i});\quad J=det\boldsymbol{F}=1+\boldsymbol{I}:\boldsymbol{\varepsilon}=1+\varepsilon_0;\quad J_{t\theta}=1+\varepsilon_{0\theta}+\varepsilon_{0t},\tag{11}$$

but with two distinctions: (a) the expression given by Eq.(4) for the gradient energy is used in order to correctly describe anisotropy of the interface energy; (b) the elastic energy ψ^e is multiplied by $J_{t\theta}$ in order to obtain elasticity consistent in the limit with large strain formulation, see [35]. Here, $\breve{\psi}^\theta$ is the thermal (chemical) energy localized at the interfaces, which is equal to zero in the bulk and $\tilde{\psi}^\theta$ is the thermal energy, which is related to the difference between the thermal parts of the free energies of two phases contacting across an interface; ε_0 is the volumetric strain and $\varepsilon_{0\theta}$ and ε_{0t} are its thermal and transformational parts. The Jacobian J serves the same purpose as in [33, 35]: it produces (with the correct choice of $\breve{\psi}^\theta$) the desired contribution to the spherical part of the structural stresses. While for small strains $J\simeq J_{t\theta}\simeq 1$ and $\boldsymbol{\nabla}\eta_k\simeq\boldsymbol{\nabla}_0\eta_k$, these geometric nonlinearities must be retained even for infinitesimal strains in order to receive the proper expression for the interface stresses [33]. **For example, even for negligible strains, according to Eq.(11) $dJ/d\boldsymbol{\varepsilon}=\boldsymbol{I}$, which will make the proper contribution to the interface stresses. If one would neglect small terms from the beginning rather than in the final result and use $J\simeq 1$, then $dJ/d\boldsymbol{\varepsilon}=\boldsymbol{0}$, and interface stresses $\boldsymbol{\sigma}_{st}=0$.** To evaluate stresses according to the first Eq.(10), we will use that $dJ/d\boldsymbol{\varepsilon}=\boldsymbol{I}$, $dJ_{t\theta}/d\boldsymbol{\varepsilon}=\boldsymbol{0}$ (since derivative is evaluated at fixed θ and η_i), and

$$\frac{\partial\,\psi^e}{\partial\,\boldsymbol{\varepsilon}}=\frac{\partial\psi^e}{\partial\boldsymbol{\varepsilon}_e}:\frac{\partial\boldsymbol{\varepsilon}_e}{\partial\boldsymbol{\varepsilon}}=\frac{\partial\,\psi^e}{\partial\boldsymbol{\varepsilon}_e}.\tag{12}$$

Let us designate $\boldsymbol{\zeta}_i = \boldsymbol{\nabla}\eta_i$ and $\boldsymbol{\zeta}_{0i} = \boldsymbol{\nabla}_0\eta_i$, and $a_{jk} = \boldsymbol{\zeta}_j \cdot \boldsymbol{\zeta}_k = a_{kj}$ for all k and j. Then since $\boldsymbol{\zeta}_k \cdot \boldsymbol{\zeta}_j = \boldsymbol{\zeta}_{0k} \cdot \boldsymbol{F}^{-1} \cdot \boldsymbol{F}^{-1t} \cdot \boldsymbol{\zeta}_{0i}$ and $\boldsymbol{F}^{-1} \cdot \boldsymbol{F}^{-1t} = (\boldsymbol{I} - \boldsymbol{\varepsilon} - \boldsymbol{\omega}) \cdot (\boldsymbol{I} - \boldsymbol{\varepsilon} + \boldsymbol{\omega}) \simeq \boldsymbol{I} - 2\boldsymbol{\varepsilon}$, where all products of small tensors are neglected, then $a_{jk} = \boldsymbol{\zeta}_{0j} \cdot (\boldsymbol{I} - 2\boldsymbol{\varepsilon}) \cdot \boldsymbol{\zeta}_{0k} = (\boldsymbol{I} - 2\boldsymbol{\varepsilon})\!:\!\boldsymbol{\zeta}_{0j} \otimes \boldsymbol{\zeta}_{0k} = (\boldsymbol{I} - 2\boldsymbol{\varepsilon})\!:\!\boldsymbol{\zeta}_{0k} \otimes \boldsymbol{\zeta}_{0j} = 0.5(\boldsymbol{I} - 2\boldsymbol{\varepsilon})\!:\!(\boldsymbol{\zeta}_{0j} \otimes \boldsymbol{\zeta}_{0k} + \boldsymbol{\zeta}_{0k} \otimes \boldsymbol{\zeta}_{0j})$. Then

$$\frac{\partial\, \psi^{\nabla}}{\partial\, \boldsymbol{\varepsilon}} = \frac{\partial \psi^{\nabla}}{\partial\, a_{jk}} \frac{\partial\, a_{jk}}{\partial\, \boldsymbol{\varepsilon}} = -\frac{\partial \psi^{\nabla}}{\partial\, a_{jk}} (\boldsymbol{\zeta}_{0j} \otimes \boldsymbol{\zeta}_{0k} + \boldsymbol{\zeta}_{0k} \otimes \boldsymbol{\zeta}_{0j}) = -\frac{\partial \psi^{\nabla}}{\partial\, a_{jk}} (\boldsymbol{\zeta}_j \otimes \boldsymbol{\zeta}_k + \boldsymbol{\zeta}_k \otimes \boldsymbol{\zeta}_j). \quad (13)$$

The last transition is eligible because at small strains $\boldsymbol{\nabla}\eta_i \simeq \boldsymbol{\nabla}_0\eta_i$ and is performed here to make our results compatible with the large strain theory for the limit case of isotropic interface energy [35]. Collecting all parts, we obtain

$$\boldsymbol{\sigma} = \boldsymbol{\sigma}_e + \boldsymbol{\sigma}_{st} + \boldsymbol{\sigma}_d; \qquad \boldsymbol{\sigma}_e = \rho_0 \frac{\partial\, \psi^e}{\partial\, \boldsymbol{\varepsilon}_e}; \quad (14)$$

$$\boldsymbol{\sigma}_{st} = \rho_0(\breve{\psi}^{\theta} + \psi^{\nabla})\boldsymbol{I} - \rho_0 \frac{\partial \psi^{\nabla}}{\partial\, a_{jk}} (\boldsymbol{\zeta}_j \otimes \boldsymbol{\zeta}_k + \boldsymbol{\zeta}_k \otimes \boldsymbol{\zeta}_j). \quad (15)$$

Because of the symmetry of a_{jk}, the interface stress $\boldsymbol{\sigma}_{st}$ and consequently the total stress are symmetric, as required. Since normals $\boldsymbol{k}_{0i}$ are independent of strain, anisotropy of the gradient energy does not produce any additional contribution to the interface stresses. However, it will significantly complicate the Ginzburg-Landau equations. It is evident that $\boldsymbol{F}^{-1} \cdot \boldsymbol{F}^{-1t}$ and ψ^{∇} are independent of a rigid-body rotation.

For a single order parameter one has $\psi^{\nabla} = \psi^{\nabla}(\boldsymbol{\zeta} \cdot \boldsymbol{\zeta}, \boldsymbol{k}_0)$. We will use below the most popular expression

$$\rho_0 \psi^{\nabla} = 0.5\beta^2(\boldsymbol{k}_0)|\boldsymbol{\nabla}\eta|^2 \quad (16)$$

and obtain from Eq.(15)

$$\boldsymbol{\sigma}_{st} = (\rho_0 \breve{\psi}^{\theta} + 0.5\beta^2(\boldsymbol{k}_0)|\boldsymbol{\nabla}\eta|^2)\boldsymbol{I} - \beta^2(\boldsymbol{k}_0)\boldsymbol{\nabla}\eta \otimes \boldsymbol{\nabla}\eta =$$
$$\beta^2(\boldsymbol{k}_0)|\boldsymbol{\nabla}\eta|^2\,(\boldsymbol{I} - \boldsymbol{k} \otimes \boldsymbol{k}) + (\rho_0 \breve{\psi}^{\theta} - 0.5\beta^2(\boldsymbol{k}_0)|\boldsymbol{\nabla}\eta|^2)\boldsymbol{I}. \quad (17)$$

The only difference between Eq.(17) and its isotropic counterpart is the dependence of the gradient coefficient β^2 on the interface orientation $\boldsymbol{k}_0$ in the undeformed state. That is why

we will pursue exactly the same approach as in [33, 35] to prove that one can chose function $\breve{\psi}^{\theta}$ in a way that for the nonequilibrium interface the last term in Eq.(17) disappears and interface stresses represent the biaxial tension (Fig. 1a) with the resultant force equal to the interface energy.

V. GINZBURG-LANDAU EQUATION

A. General expression

The usual linear relationships $\dot{\eta}_i = L_{ij}X_j$ with positive definite kinetic coefficients L_{ij}, for which the Onsager reciprocal relationships $L_{ij} = L_{ji}$ are met, and together with the **second** Eq.(10) lead to the generalized Ginzburg-Landau equation

$$\dot{\eta}_j = L_{ji}\left(-\frac{\partial\bar{\psi}}{\partial\eta_i} + \boldsymbol{\nabla}_0 \cdot \frac{\partial\bar{\psi}}{\partial\boldsymbol{\nabla}_0\eta_i}\right). \tag{18}$$

The local term in the driving force in Eq.(18) was evaluated in [35]:

$$-\frac{\partial\bar{\psi}}{\partial\eta_i} = \frac{\boldsymbol{\sigma}_e}{\rho_0}\!:\!\frac{\partial\boldsymbol{\varepsilon}_\theta(\theta,\eta_k)}{\partial\eta_i} + \frac{\boldsymbol{\sigma}_e}{\rho_0}\!:\!\frac{\partial\boldsymbol{\varepsilon}_t(\eta_k)}{\partial\eta_i} - \frac{1}{\rho_0}\frac{\partial\psi^e}{\partial\eta_i}\Big|_{\boldsymbol{\varepsilon}_e} - \frac{\psi^e}{\rho_0}\left(\frac{\partial\boldsymbol{\varepsilon}_{t0}}{\partial\eta_i} + \frac{\partial\boldsymbol{\varepsilon}_{\theta 0}}{\partial\eta_i}\right) - \frac{\partial\breve{\psi}^{\theta}}{\partial\eta_i} - \frac{\partial\tilde{\psi}^{\theta}}{\partial\eta_i}. \tag{19}$$

Allowing for the Jacobian $J_{t\theta}$ in front of the elastic energy in Eq.(11) resulted in an additional term in Eq.(19), which was absent in the small strain formulation in [33]. The interface stresses do not explicitly appear in the Ginzburg-Landau equation. However, they affect the distribution of the elastic stresses and indirectly contribute to Eq.(19).

The most commonly used *boundary condition* for the order parameter is [33, 35]

$$\boldsymbol{n}\cdot\boldsymbol{Q}_i^{\eta} = \boldsymbol{n}\cdot\rho_0\frac{\partial\psi}{\partial\boldsymbol{\nabla}\eta_i} = H_i, \tag{20}$$

where H_i are given functions, in particular, those related to change in the surface energy during PT, and $\boldsymbol{n}$ is the unit normal to the external surface. Alternatively, one can use periodic boundary conditions, or a prescribed value of η_i, or consider a finite-width external surface [55, 56] which results in a number of interesting scale and mechanics effects.

B. Previous theory

Below we will consider a single order parameter for simplicity . The most common choice for the gradient energy (e.g., in [38, 39]) is $\rho_0\psi^\nabla = 0.5\beta^2(\boldsymbol{k})|\boldsymbol{\nabla}\eta|^2 = 0.5\beta^2(\boldsymbol{\nabla}\eta) = 0.5\beta^2(\boldsymbol{\zeta})$, where the homogeneous degree one function $\beta(\boldsymbol{\nabla}\eta) = |\boldsymbol{\nabla}\eta|\beta(\boldsymbol{k})$. Then

$$\rho_0\frac{\partial\psi^\nabla}{\partial\boldsymbol{\nabla}\eta} = \beta(\boldsymbol{\nabla}\eta)\frac{\partial\beta(\boldsymbol{\nabla}\eta)}{\partial\boldsymbol{\nabla}\eta} = \beta(\boldsymbol{\zeta})\frac{\partial\beta(\boldsymbol{\zeta})}{\partial\boldsymbol{\zeta}} \tag{21}$$

and the analog of the Ginzburg-Landau equation (18) in the deformed state is

$$\dot\eta = L\left(-\frac{\partial\bar\psi}{\partial\eta} + \boldsymbol{\nabla}\cdot\left(\frac{\partial\bar\psi}{\partial\boldsymbol{\nabla}\eta}\right)\right) = L\left(-\frac{\partial\bar\psi}{\partial\eta} + \frac{1}{\rho}\left(\frac{\partial\beta}{\partial\zeta_k}\frac{\partial\beta}{\partial\zeta_i} + \beta\frac{\partial^2\beta}{\partial\zeta_k\partial\zeta_i}\right)\frac{\partial^2\eta}{\partial r_k\partial r_i}\right) =$$
$$L\left(-\frac{\partial\bar\psi}{\partial\eta} + \frac{1}{\rho}\left(\frac{\partial\beta}{\partial\boldsymbol{\zeta}}\otimes\frac{\partial\beta}{\partial\boldsymbol{\zeta}} + \beta\frac{\partial^2\beta}{\partial\boldsymbol{\zeta}\partial\boldsymbol{\zeta}}\right)\vdots\frac{\partial^2\eta}{\partial\boldsymbol{r}\partial\boldsymbol{r}}\right). \tag{22}$$

C. Current theory

Using the function $\beta(\boldsymbol{\nabla}_0\eta) = |\boldsymbol{\nabla}_0\eta|\beta(\boldsymbol{k}_0)$, we present the gradient energy (16) in the form

$$\rho_0\psi^\nabla = 0.5(\beta(\boldsymbol{k}_0)|\boldsymbol{\zeta}|)^2 = 0.5\left(\beta(\boldsymbol{\zeta}_0)\frac{|\boldsymbol{\zeta}|}{|\boldsymbol{\zeta}_0|}\right)^2 \tag{23}$$
$$= 0.5\beta^2(\boldsymbol{\zeta}_0)\frac{\boldsymbol{\zeta}_0\cdot\boldsymbol{F}^{-1}\cdot\boldsymbol{F}^{-1T}\cdot\boldsymbol{\zeta}_0}{\boldsymbol{\zeta}_0\cdot\boldsymbol{\zeta}_0} = 0.5\beta^2(\boldsymbol{\zeta}_0)\frac{\boldsymbol{\zeta}_0\cdot(\boldsymbol{I}-2\boldsymbol{\varepsilon})\cdot\boldsymbol{\zeta}_0}{\boldsymbol{\zeta}_0\cdot\boldsymbol{\zeta}_0}.$$

Then we evaluate

$$\boldsymbol{Q}^\eta = \rho_0\frac{\partial\psi^\nabla}{\partial\boldsymbol{\nabla}_0\eta} = \rho_0\frac{\partial\psi^\nabla}{\partial\boldsymbol{\zeta}_0} = \beta(\boldsymbol{\zeta}_0)\frac{\partial\beta(\boldsymbol{\zeta}_0)}{\partial\boldsymbol{\zeta}_0} -$$
$$2\beta(\boldsymbol{\zeta}_0)\frac{\partial\beta(\boldsymbol{\zeta}_0)}{\partial\boldsymbol{\zeta}_0}\frac{\boldsymbol{\zeta}_0\cdot\boldsymbol{\varepsilon}\cdot\boldsymbol{\zeta}_0}{\boldsymbol{\zeta}_0\cdot\boldsymbol{\zeta}_0} + 2\beta^2(\boldsymbol{\zeta}_0)\frac{\boldsymbol{\zeta}_0}{\boldsymbol{\zeta}_0\cdot\boldsymbol{\zeta}_0}\cdot\left(\boldsymbol{I}\frac{\boldsymbol{\zeta}_0\cdot\boldsymbol{\varepsilon}\cdot\boldsymbol{\zeta}_0}{\boldsymbol{\zeta}_0\cdot\boldsymbol{\zeta}_0} - \boldsymbol{\varepsilon}\right), \tag{24}$$

or in the component form in the Cartesian coordinate system:

$$Q_i^\eta = \rho_0\frac{\partial\psi^\nabla}{\partial(\partial\eta/\partial r_{0i})} = \rho_0\frac{\partial\psi^\nabla}{\partial\zeta_{0i}} = \beta(\boldsymbol{\zeta}_0)\frac{\partial\beta(\boldsymbol{\zeta}_0)}{\partial\zeta_{0i}} - 2\beta(\boldsymbol{\zeta}_0)\frac{\partial\beta(\boldsymbol{\zeta}_0)}{\partial\zeta_{0i}}\frac{\varepsilon_{bc}\zeta_{0b}\zeta_{0c}}{\zeta_{0a}\zeta_{0a}}$$
$$-2\beta^2(\boldsymbol{\zeta}_0)\frac{\zeta_{0b}}{\zeta_{0a}\zeta_{0a}}\left[\varepsilon_{ib} - \delta_{ib}\frac{\varepsilon_{sc}\zeta_{0s}\zeta_{0c}}{\zeta_{0a}\zeta_{0a}}\right]. \tag{25}$$

These expressions for $\boldsymbol{Q}^{\eta}$ should be used in the boundary conditions (20). The explicit expression for the Ginzburg-Landau equation can be presented in the component form

$$\frac{\rho_0\dot{\eta}}{L}=-\rho_0\frac{\partial\bar{\psi}}{\partial\eta}+\left(\frac{\partial\beta}{\partial\zeta_{0k}}\frac{\partial\beta}{\partial\zeta_{0i}}+\beta\frac{\partial^2\beta}{\partial\zeta_{0k}\partial\zeta_{0i}}\right)\frac{\partial^2\eta}{\partial r_{0k}\partial r_{0i}}\frac{(\delta_{bc}-2\varepsilon_{bc})\zeta_{0b}\zeta_{0c}}{\zeta_{0a}\zeta_{0a}}+$$
$$2\beta\frac{\partial\beta}{\partial\zeta_{0i}}\left(-\frac{\frac{\partial\varepsilon_{bc}}{\partial r_{0i}}\zeta_{0b}\zeta_{0c}+4\varepsilon_{bc}\frac{\partial^2\eta}{\partial r_{0b}\partial r_{0i}}\zeta_{0c}}{\zeta_{0a}\zeta_{0a}}+\frac{4\varepsilon_{bc}\zeta_{0b}\zeta_{0c}\zeta_{0a}\frac{\partial^2\eta}{\partial r_{0a}\partial r_{0i}}}{(\zeta_{0a}\zeta_{0a})^2}\right)$$
$$-2\beta^2\left(\frac{\frac{\partial\varepsilon_{ib}}{\partial r_{0i}}\zeta_{0b}+\varepsilon_{ib}\frac{\partial^2\eta}{\partial r_{0b}\partial r_{0i}}}{\zeta_{0a}\zeta_{0a}}-\frac{4\varepsilon_{ib}\zeta_{0b}\zeta_{0a}\frac{\partial^2\eta}{\partial r_{0a}\partial r_{0i}}}{(\zeta_{0a}\zeta_{0a})^2}\right)$$
$$+2\beta^2\left(\frac{\frac{\partial\varepsilon_{bc}}{\partial r_{0i}}\zeta_{0i}\zeta_{0b}\zeta_{0c}+\frac{\partial^2\eta}{\partial r_{0i}\partial r_{0i}}\varepsilon_{bc}\zeta_{0b}\zeta_{0c}}{(\zeta_{0a}\zeta_{0a})^2}-4\frac{\zeta_{0i}\varepsilon_{bc}\zeta_{0b}\zeta_{0c}\zeta_{0a}\frac{\partial^2\eta}{\partial r_{0a}\partial r_{0i}}}{(\zeta_{0a}\zeta_{0a})^3}\right), \tag{26}$$

or in direct tensor notations

$$\frac{\rho_0\dot{\eta}}{L}=-\rho_0\frac{\partial\bar{\psi}}{\partial\eta}+\left(\frac{\partial\beta}{\partial\boldsymbol{\zeta}_0}\otimes\frac{\partial\beta}{\partial\boldsymbol{\zeta}_0}+\beta\frac{\partial^2\beta}{\partial\boldsymbol{\zeta}_0\partial\boldsymbol{\zeta}_0}\right)\vdots\frac{\partial^2\eta}{\partial\boldsymbol{r}_0\partial\boldsymbol{r}_0}\,\frac{\boldsymbol{\zeta}_0\cdot(\boldsymbol{I}-2\boldsymbol{\varepsilon})\cdot\boldsymbol{\zeta}_0}{\boldsymbol{\zeta}_0\cdot\boldsymbol{\zeta}_0}+$$
$$2\beta\frac{\partial\beta}{\partial\boldsymbol{\zeta}_0}\cdot\left(-\frac{\boldsymbol{\zeta}_0\otimes\boldsymbol{\zeta}_0\vdots\frac{\partial\boldsymbol{\varepsilon}}{\partial\boldsymbol{r}_0}+4\frac{\partial^2\eta}{\partial\boldsymbol{r}_0\partial\boldsymbol{r}_0}\cdot\boldsymbol{\varepsilon}\cdot\boldsymbol{\zeta}_0}{|\boldsymbol{\zeta}_0|^2}+\frac{4\boldsymbol{\zeta}_0\cdot\boldsymbol{\varepsilon}\cdot\boldsymbol{\zeta}_0\boldsymbol{\zeta}_0\cdot\frac{\partial^2\eta}{\partial\boldsymbol{r}_0\partial\boldsymbol{r}_0}}{|\boldsymbol{\zeta}_0|^4}\right)$$
$$-2\beta^2\left(\frac{\boldsymbol{\zeta}_0\cdot\frac{\partial\boldsymbol{\varepsilon}}{\partial\boldsymbol{r}_0}\vdots\boldsymbol{I}+\boldsymbol{\varepsilon}\vdots\frac{\partial^2\eta}{\partial\boldsymbol{r}_0\partial\boldsymbol{r}_0}}{|\boldsymbol{\zeta}_0|^2}-\frac{4\left(\boldsymbol{\varepsilon}\cdot\boldsymbol{\zeta}_0\right)\cdot\left(\boldsymbol{\zeta}_0\cdot\frac{\partial^2\eta}{\partial\boldsymbol{r}_0\partial\boldsymbol{r}_0}\right)}{|\boldsymbol{\zeta}_0|^4}\right)$$
$$+2\beta^2\left(\frac{\boldsymbol{\zeta}_0\otimes\boldsymbol{\zeta}_0\vdots\frac{\partial\boldsymbol{\varepsilon}}{\partial\boldsymbol{r}_0}\cdot\boldsymbol{\zeta}_0+\nabla_0^2\eta\boldsymbol{\zeta}_0\cdot\boldsymbol{\varepsilon}\cdot\boldsymbol{\zeta}_0}{|\boldsymbol{\zeta}_0|^4}-4\frac{\boldsymbol{\zeta}_0\cdot\boldsymbol{\varepsilon}\cdot\boldsymbol{\zeta}_0\boldsymbol{\zeta}_0\otimes\boldsymbol{\zeta}_0\vdots\frac{\partial^2\eta}{\partial\boldsymbol{r}_0\partial\boldsymbol{r}_0}}{|\boldsymbol{\zeta}_0|^6}\right). \tag{27}$$

In these equations β is considered as a homogeneous degree one function of $\boldsymbol{\zeta}_0$ rather than of unit normal $\boldsymbol{k}_0$. One can also neglect $2\boldsymbol{\varepsilon}$ in comparison with $\boldsymbol{I}$.

For a linear elastic material we set

$$\rho_0\psi^e=0.5\boldsymbol{\varepsilon}_e\vdots\boldsymbol{C}(\eta)\vdots\boldsymbol{\varepsilon}_e;\qquad\boldsymbol{\sigma}_e=\boldsymbol{C}(\eta)\vdots\boldsymbol{\varepsilon}_e, \tag{28}$$

i.e., Hooke's law, where $\boldsymbol{C}$ is the fourth-rank tensor of elastic moduli, which is different in different phases. We substitute Hooke's law in Eqs.(19) and (27) and will evaluate the degree of smallness of each strain-related term in the right-hand side of the Ginzburg-Landau

equation. We will do this under the assumption that usually elastic and thermal strains are at least an order of magnitude lower than the transformation and total strains, i.e., $\boldsymbol{\varepsilon}_e \sim \boldsymbol{\varepsilon}_\theta \sim \boldsymbol{\varepsilon}_t^2 \sim \boldsymbol{\varepsilon}^2$. In this case we find that

– the terms due to anisotropy of the interface energy are proportional to $\boldsymbol{\varepsilon}$, i.e. they are of the first order of smallness for a small magnitude of $\boldsymbol{\varepsilon}$;

– the work of stresses on the change in the transformation strain is proportional to $\boldsymbol{\varepsilon}^3$;

– the stress work on the thermal strain and the term related to change in elastic moduli are proportional to $\boldsymbol{\varepsilon}^4$;

– and the term proportional to the elastic energy ψ^e is proportional to $\boldsymbol{\varepsilon}_t^5$ and $\boldsymbol{\varepsilon}_\theta^6$.

Thus, unexpectedly, the first order correction in the Ginzburg-Landau equation due to infinitesimal strains is related to our correction due to the anisotropic gradient energy rather than due to traditional transformation work. Such an analysis is strict for infinitesimal $\boldsymbol{\varepsilon}$. For small but finite $\boldsymbol{\varepsilon}$ the magnitude of each of this term depends on the corresponding coefficients, which may alter our conclusions. If one neglects all the terms with strains that appeared due to anisotropy of the gradient energy, Eqs.(26) and (27) reduce to Eq.(22).

VI. COMPLETE SYSTEM OF EQUATIONS FOR A SINGLE ORDER PARAMETER

Below we collect the complete system of equations for a single order parameter and the anisotropic interface energy. Some functions and equations (e.g., $\breve{\psi}^\theta$ and $\tilde{\psi}^\theta$) are taken from [33]. It will be shown in the next Section that they are consistent with the analytical solution for a propagating interface and biaxial interface stresses, as in [33] for isotropic interface energy.

1. Kinematics

1.1. Decomposition of the strain tensor $\boldsymbol{\varepsilon}$; volumetric strains

$$\boldsymbol{\varepsilon} = (\boldsymbol{\nabla}_0 \boldsymbol{u})_s; \quad \boldsymbol{\varepsilon} = \boldsymbol{\varepsilon}_e + \boldsymbol{\varepsilon}_t(\eta) + \boldsymbol{\varepsilon}_\theta(\theta, \eta);$$

$$J = det\boldsymbol{F} = \frac{\rho_0}{\rho} = 1 + \boldsymbol{I}{:}\boldsymbol{\varepsilon} = 1 + \varepsilon_0; \quad J_{t\theta} = 1 + \varepsilon_{0\theta} + \varepsilon_{0t}. \tag{29}$$

1.2. Transformation $\boldsymbol{\varepsilon}_t$ and thermal $\boldsymbol{\varepsilon}_\theta$ strains

$$\boldsymbol{\varepsilon}_t = \bar{\boldsymbol{\varepsilon}}_t\, \varphi(a,\eta); \qquad \boldsymbol{\varepsilon}_\theta = \boldsymbol{\varepsilon}_{\theta H} + (\boldsymbol{\varepsilon}_{\theta L} - \boldsymbol{\varepsilon}_{\theta H})\, \varphi(a_\theta,\eta);$$
$$\varphi(a,\eta) = a\eta^2(1-\eta)^2 + (4\eta^3 - 3\eta^4). \tag{30}$$

2. Helmholtz free energy per unit mass and its contributions

$$\bar{\psi}(\boldsymbol{\varepsilon},\eta,\theta,\boldsymbol{\zeta},\boldsymbol{\zeta}_0) = \psi^e + J\breve{\psi}^\theta + \tilde{\psi}^\theta + J\psi^\nabla; \quad \boldsymbol{\zeta}_0 = \boldsymbol{\nabla}_0\eta; \quad \boldsymbol{\zeta} = \boldsymbol{\nabla}\eta; \tag{31}$$
$$\breve{\psi}^\theta = (A(\theta) - 3\Delta\, G^\theta(\theta))\eta^2(1-\eta)^2; \quad \tilde{\psi}^\theta = \Delta\, G^\theta(\theta)\eta^2(3-2\eta);$$
$$\psi^e = \frac{1}{2\rho_0}\boldsymbol{\varepsilon}_e{:}\boldsymbol{C}(\eta){:}\boldsymbol{\varepsilon}_e; \qquad \boldsymbol{C}(\eta) = \boldsymbol{C}_H + (\boldsymbol{C}_L - \boldsymbol{C}_H)\varphi(a_C,\eta). \tag{32}$$

$$\rho_0\psi^\nabla = 0.5(\beta(\boldsymbol{k}_0)|\boldsymbol{\zeta}|)^2 = 0.5\left(\beta(\boldsymbol{\zeta}_0)\frac{|\boldsymbol{\zeta}|}{|\boldsymbol{\zeta}_0|}\right)^2 = 0.5\beta^2(\boldsymbol{\zeta}_0)\frac{\boldsymbol{\zeta}_0\cdot(\boldsymbol{I}-2\boldsymbol{\varepsilon})\cdot\boldsymbol{\zeta}_0}{\boldsymbol{\zeta}_0\cdot\boldsymbol{\zeta}_0}. \tag{33}$$

3. Stress tensor

$$\boldsymbol{\sigma} = \boldsymbol{\sigma}_e + \boldsymbol{\sigma}_{st} + \boldsymbol{\sigma}_d; \tag{34}$$
$$\boldsymbol{\sigma}_e = \rho_0\frac{\partial\,\psi^e}{\partial\,\boldsymbol{\varepsilon}_e} = \boldsymbol{C}(\eta){:}\boldsymbol{\varepsilon}_e; \quad \boldsymbol{\sigma}_d = \boldsymbol{B}{:}\dot{\boldsymbol{\varepsilon}};$$
$$\boldsymbol{\sigma}_{st} = \beta^2(\boldsymbol{k}_0)|\boldsymbol{\nabla}\eta|^2\,(\boldsymbol{I} - \boldsymbol{k}\otimes\boldsymbol{k}) + (\rho_0\breve{\psi}^\theta - 0.5\beta^2(\boldsymbol{k}_0)|\boldsymbol{\nabla}\eta|^2)\boldsymbol{I}. \tag{35}$$

4. Ginzburg–Landau equation

4.1. Coupled with mechanics

$$\frac{\rho_0\dot{\eta}}{L(\boldsymbol{k}_0)} = -\rho_0\frac{\partial\bar{\psi}}{\partial\eta} + \left(\frac{\partial\beta}{\partial\boldsymbol{\zeta}_0}\otimes\frac{\partial\beta}{\partial\boldsymbol{\zeta}_0} + \beta\frac{\partial^2\beta}{\partial\boldsymbol{\zeta}_0\partial\boldsymbol{\zeta}_0}\right){:}\frac{\partial^2\eta}{\partial\boldsymbol{r}_0\partial\boldsymbol{r}_0}\,\frac{\boldsymbol{\zeta}_0\cdot(\boldsymbol{I}-2\boldsymbol{\varepsilon})\cdot\boldsymbol{\zeta}_0}{\boldsymbol{\zeta}_0\cdot\boldsymbol{\zeta}_0} +$$
$$2\beta\frac{\partial\beta}{\partial\boldsymbol{\zeta}_0}\cdot\left(-\frac{\boldsymbol{\zeta}_0\otimes\boldsymbol{\zeta}_0{:}\frac{\partial\boldsymbol{\varepsilon}}{\partial\boldsymbol{r}_0} + 4\frac{\partial^2\eta}{\partial\boldsymbol{r}_0\partial\boldsymbol{r}_0}\cdot\boldsymbol{\varepsilon}\cdot\boldsymbol{\zeta}_0}{|\boldsymbol{\zeta}_0|^2} + \frac{4\boldsymbol{\zeta}_0\cdot\boldsymbol{\varepsilon}\cdot\boldsymbol{\zeta}_0\boldsymbol{\zeta}_0\cdot\frac{\partial^2\eta}{\partial\boldsymbol{r}_0\partial\boldsymbol{r}_0}}{|\boldsymbol{\zeta}_0|^4}\right)$$
$$-2\beta^2\left(\frac{\boldsymbol{\zeta}_0\cdot\frac{\partial\boldsymbol{\varepsilon}}{\partial\boldsymbol{r}_0}{:}\boldsymbol{I} + \boldsymbol{\varepsilon}{:}\frac{\partial^2\eta}{\partial\boldsymbol{r}_0\partial\boldsymbol{r}_0}}{|\boldsymbol{\zeta}_0|^2} - \frac{4\,(\boldsymbol{\varepsilon}\cdot\boldsymbol{\zeta}_0)\cdot\left(\boldsymbol{\zeta}_0\cdot\frac{\partial^2\eta}{\partial\boldsymbol{r}_0\partial\boldsymbol{r}_0}\right)}{|\boldsymbol{\zeta}_0|^4}\right)$$
$$+2\beta^2\left(\frac{\boldsymbol{\zeta}_0\otimes\boldsymbol{\zeta}_0{:}\frac{\partial\boldsymbol{\varepsilon}}{\partial\boldsymbol{r}_0}\cdot\boldsymbol{\zeta}_0 + \nabla_0^2\eta\boldsymbol{\zeta}_0\cdot\boldsymbol{\varepsilon}\cdot\boldsymbol{\zeta}_0}{|\boldsymbol{\zeta}_0|^4} - 4\frac{\boldsymbol{\zeta}_0\cdot\boldsymbol{\varepsilon}\cdot\boldsymbol{\zeta}_0\boldsymbol{\zeta}_0\otimes\boldsymbol{\zeta}_0{:}\frac{\partial^2\eta}{\partial\boldsymbol{r}_0\partial\boldsymbol{r}_0}}{|\zeta_0|^6}\right). \tag{36}$$

$$-\rho_0\frac{\partial\bar{\psi}}{\partial\eta}=\boldsymbol{\sigma}_e\!:\!\frac{\partial\boldsymbol{\varepsilon}_\theta(\theta,\eta_k)}{\partial\eta}+\boldsymbol{\sigma}_e\!:\!\frac{\partial\boldsymbol{\varepsilon}_t(\eta)}{\partial\eta}-\frac{\partial\psi^e}{\partial\eta}\Big|_{\boldsymbol{\varepsilon}_e}-\psi^e\left(\frac{\partial\boldsymbol{\varepsilon}_{t0}}{\partial\eta}+\frac{\partial\boldsymbol{\varepsilon}_{\theta0}}{\partial\eta}\right)-\rho_0\frac{\partial\breve{\psi}^\theta}{\partial\eta}-\rho_0\frac{\partial\tilde{\psi}^\theta}{\partial\eta} \tag{37}$$

4.2. Without strains and elastic stresses

$$\frac{\rho_0\dot{\eta}}{L(\boldsymbol{k})}=-\rho_0\frac{\partial(\breve{\psi}^\theta+\tilde{\psi}^\theta)}{\partial\eta}+\left(\frac{\partial\beta}{\partial\boldsymbol{\zeta}_0}\otimes\frac{\partial\beta}{\partial\boldsymbol{\zeta}_0}+\beta\frac{\partial^2\beta}{\partial\boldsymbol{\zeta}_0\partial\boldsymbol{\zeta}_0}\right)\!:\!\frac{\partial^2\eta}{\partial\boldsymbol{r}_0\partial\boldsymbol{r}_0} \tag{38}$$

4.3. For interface propagating along the fixed normal $\boldsymbol{k}$

$$\rho_0\psi^\nabla=0.5\left(\beta(\boldsymbol{k})\frac{d\eta}{dx}\right)^2;\qquad\dot{\eta}=\bar{L}(\boldsymbol{k})\left(-\rho_0\frac{\partial(\breve{\psi}^\theta+\tilde{\psi}^\theta)}{\partial\eta}+\beta^2(\boldsymbol{k})\frac{\partial^2\eta}{\partial x^2}\right);\qquad\bar{L}=L/\rho_0 \tag{39}$$

5. Gradient energy coefficient for cubic crystals

$$\beta(\boldsymbol{k}_0)=\alpha_0+\alpha_1\frac{\zeta_{0i}^2\zeta_{0j}^2+\zeta_{0i}^2\zeta_{0k}^2+\zeta_{0k}^2\zeta_{0j}^2}{|\boldsymbol{\zeta}_0|^4}+\alpha_2\frac{\zeta_{0i}^2\zeta_{0j}^2\zeta_{0k}^2}{|\boldsymbol{\zeta}_0|^6}+\alpha_3\frac{\left(\zeta_{0i}^2\zeta_{0j}^2+\zeta_{0i}^2\zeta_{0k}^2+\zeta_{0k}^2\zeta_{0j}^2\right)^2}{|\boldsymbol{\zeta}_0|^8} \tag{40}$$

$$\beta(\boldsymbol{\zeta}_0)=\alpha_0|\boldsymbol{\zeta}_0|+\alpha_1\frac{\zeta_{0i}^2\zeta_{0j}^2+\zeta_{0i}^2\zeta_{0k}^2+\zeta_{0k}^2\zeta_{0j}^2}{|\boldsymbol{\zeta}_0|^3}+\alpha_2\frac{\zeta_{0i}^2\zeta_{0j}^2\zeta_{0k}^2}{|\boldsymbol{\zeta}_0|^5}+\alpha_3\frac{\left(\zeta_{0i}^2\zeta_{0j}^2+\zeta_{0i}^2\zeta_{0k}^2+\zeta_{0k}^2\zeta_{0j}^2\right)^2}{|\boldsymbol{\zeta}_0|^7} \tag{41}$$

6. Linear momentum balance equation

$$\nabla\cdot\boldsymbol{\sigma}=\rho_0\dot{\boldsymbol{v}}\,, \tag{42}$$

7. Boundary conditions for the order parameter

$$\boldsymbol{n}\cdot\rho_0\frac{\partial\psi}{\partial\boldsymbol{\nabla}\eta}=H;\qquad\rho_0\frac{\partial\psi^\nabla}{\partial\boldsymbol{\nabla}_0\eta}=\rho_0\frac{\partial\psi^\nabla}{\partial\boldsymbol{\zeta}_0}=\beta(\boldsymbol{\zeta}_0)\frac{\partial\beta(\boldsymbol{\zeta}_0)}{\partial\boldsymbol{\zeta}_0}-$$
$$2\beta(\boldsymbol{\zeta}_0)\frac{\partial\beta(\boldsymbol{\zeta}_0)}{\partial\boldsymbol{\zeta}_0}\frac{\boldsymbol{\zeta}_0\cdot\boldsymbol{\varepsilon}\cdot\boldsymbol{\zeta}_0}{\boldsymbol{\zeta}_0\cdot\boldsymbol{\zeta}_0}+2\beta^2(\boldsymbol{\zeta}_0)\frac{\boldsymbol{\zeta}_0}{\boldsymbol{\zeta}_0\cdot\boldsymbol{\zeta}_0}\cdot\left(\boldsymbol{I}\frac{\boldsymbol{\zeta}_0\cdot\boldsymbol{\varepsilon}\cdot\boldsymbol{\zeta}_0}{\boldsymbol{\zeta}_0\cdot\boldsymbol{\zeta}_0}-\boldsymbol{\varepsilon}\right),$$

8. Expression for entropy

$$s=\frac{1}{\rho_0}\boldsymbol{\sigma}_e\!:\!\frac{\partial\boldsymbol{\varepsilon}_\theta}{\partial\theta}-\frac{1}{\rho_0}\frac{\partial\psi^e}{\partial\theta}\Big|_{\boldsymbol{\varepsilon}_e}-\frac{1}{\rho_0}\psi^e\frac{\partial J_\theta}{\partial\theta}-\frac{\partial\breve{\psi}^\theta}{\partial\theta}-\frac{\partial\tilde{\psi}^\theta}{\partial\theta}-\frac{\partial\beta^2(\theta,\boldsymbol{k}_0)}{\partial\theta}\frac{1}{2\rho_0}|\boldsymbol{\nabla}\eta|^2. \tag{43}$$

The function $\beta(\boldsymbol{k}_0)$ in Eq.(40) is obtained based on the proportionality $\beta(\boldsymbol{k}_0)=\gamma(\boldsymbol{k}_0)Z$ (see Eq.(49) below where a factor Z is defined) and the function $\gamma(\boldsymbol{k}_0)$ suggested in [57]. Specific parameters α_i were calibrated in [57] for two dozen cubic metals using molecular dynamics simulations. In Eqs.(40) and (41) $i\neq j\neq k$ and there is no summation over these

indices. The components of $\boldsymbol{k}_0$ or $\boldsymbol{\zeta}_0$ can be treated as Miller indices of crystallographic planes. Derivatives of $\beta(\boldsymbol{\zeta}_0)$ are given in the Appendix. Eq.(39) is written in order to study an interface propagating in an arbitrary chosen direction of the interface normal $\boldsymbol{k}$. The axis x of the Cartesian coordinate system is directed along $\boldsymbol{k}$ and the problem is one-dimensional and without mechanics. However, interface stresses (which do not affect Eq.(39)) will be determined. An interface rotation toward the interface energy minimum is forbidden by fixing $\boldsymbol{k}$. This will allow us to find the interface parameters for an arbitrary $\boldsymbol{k}$ and calibrate interface properties by comparing them with corresponding molecular dynamic simulations in [57]. Eq.(43) is obtained similarly to that in [33, 35] but for anisotropic β. The third term was absent in [33] but appeared in [35], where large strain formulation was simplified for small strains.

VII. A PROPAGATING INTERFACE: STRUCTURE, ENERGY, WIDTH, AND STRESSES

Our goal here is to show that all results obtained in [33] for isotropic interface energy (an analytical solution for the propagating interface and critical nucleus, an expression for the parts $\breve{\psi}^\theta$ and $\tilde{\psi}^\theta$ of the free energy that result in biaxial interface tension with the resultant force equal to the nonequilibrium interface energy, as well as expressions for the interface energy and width) can be easily generalized for the anisotropic gradient energy Eq.(16). In particular, functions $\breve{\psi}^\theta$ and $\tilde{\psi}^\theta$ remain the same as for isotropic interface energy. That is why we will take them from [33] and prove that they are correct for anisotropic interface energy rather than derive them as in [33]. At the same time, our result will generalize some known results [37, 38, 57] for the anisotropic equilibrium interface for the anisotropic propagating interface, in particular, they determine orientation dependence of the interface energy and width in terms of $\beta(\boldsymbol{k}_0)$ (due to negligible strains, $\beta(\boldsymbol{k}_0) \simeq \beta(\boldsymbol{k})$). **Obtained equations allow one to calibrate orientation-dependent material functions**

in our model in terms of measurable (or calculated in atomistic simulations) orientation-dependent interface energy, width, and mobility.

Analytical solution. The structure of a propagating plane interface is described by the same analytical solution to Eq.(39) as in [33, 58]:

$$\eta_{in} = (1 + e^{-\zeta})^{-1}; \quad \zeta = k(\boldsymbol{k})(x - ct) \quad k(\boldsymbol{k}) = \sqrt{2B}/\beta(\boldsymbol{k}); \quad B := \rho_0(A(\theta) - 3\Delta\, G^\theta(\theta)) \tag{44}$$

but with parameters depending on propagation direction $\boldsymbol{k}$. The interface velocity, c, and width, δ, are:

$$c(\boldsymbol{k}) = 6\bar{L}\rho_0\Delta\, G^\theta(\theta)/k(\boldsymbol{k}); \quad \delta(\boldsymbol{k}) = 10/k(\boldsymbol{k}). \tag{45}$$

An important property of the solution Eq.(44), $d\eta_{in}/d\zeta = \eta_{in}(1 - \eta_{in})$, combined with the definition of $k(\boldsymbol{k})$ in Eq.(44) yields the key relationship for the points of a propagating interface:

$$\psi^\nabla = \frac{\beta^2(\boldsymbol{k})}{2\rho_0}|\boldsymbol{\nabla}\eta_{in}|^2 = \frac{\beta^2(\boldsymbol{k})k^2(\boldsymbol{k})}{2\rho_0}\left(\frac{d\eta_{in}}{d\zeta}\right)^2 = (A(\theta) - 3\Delta\, G^\theta(\theta))\eta_{in}^2(1 - \eta_{in})^2 = \breve{\psi}^\theta, \tag{46}$$

where definition for $\breve{\psi}^\theta$ from Eq.(32) was used. Substitution of this identity in Eq.(35) for the interface stresses eliminates the last term and results in a biaxial tension (Fig. 1a):

$$\boldsymbol{\sigma}_{st} = \sigma_{st}\,(\boldsymbol{I} - \boldsymbol{k} \otimes \boldsymbol{k})\,; \quad \sigma_{st} = \beta^2(\boldsymbol{k})|\boldsymbol{\nabla}\eta|^2 = 2\rho_0\breve{\psi}^\theta \tag{47}$$

with σ_{st} for the magnitude of the interface stress. This confirms correctness of the definition of $\breve{\psi}^\theta$ in Eq.(32).

Nonequilibrium interface energy and width. By the definition of the interface energy under the nonequilibrium condition (see, e.g., [19]), it is equal to the excess energy with respect to H in the region with H phase $x \le x_i$ and with respect to L in the region with L phase $x > x_i$:

$$\gamma := \int_{-\infty}^{x_i} \rho_0(\psi - \psi_H)dx + \int_{x_i}^{\infty} \rho_0(\psi - \psi_L)dx. \tag{48}$$

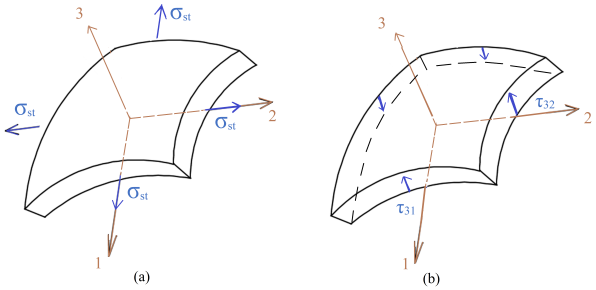

FIG. 1. Interface stresses. (a) Biaxial tension with the resultant force equal to the orientation-dependent nonequilibrium interface energy that appears in the current theory; (b) Additional artificial interface shear stresses, which are present in the previous theories and are absent in the current approach. Because shear stresses are nonsymmetric they produce artificial equilibrated torque.

Here x_i is the position of the Gibbs dividing surface (sharp interface), which was determined in [35, 36] using the principle of static equivalence. For the chosen fourth-degree thermodynamic potential, it was determined that the dividing surface corresponds to $\eta = 0.5$, which remains true for anisotropic gradient energy. Repeating the same derivations as in [33] but for anisotropic interface energy, we obtain

$$\gamma(\boldsymbol{k},\theta) = \Psi^l + \Psi^\nabla = 2\Psi^l = 2\Psi^\nabla = \frac{\beta(\boldsymbol{k},\theta)\sqrt{2B}}{6}$$
$$= \frac{k(\boldsymbol{k},\theta)\beta^2(\boldsymbol{k},\theta)}{6} = \frac{B}{3k(\boldsymbol{k},\theta)} = \frac{\rho_0(A-3\Delta G^\theta)}{3k(\boldsymbol{k},\theta)}, \tag{49}$$

where Ψ^l and Ψ^∇ are integrals of local and gradient energy, respectively. Thus, similar to the equilibrium interface, for the nonequilibrium interface the total energy is the doubled gradient energy. Since the magnitude of the interface stress is equal to the double gradient energy at each point (Eq.(47)), then the total force is equal to the double total gradient energy, which is $\gamma(\boldsymbol{k},\theta)$. Thus, the resultant force for the interface stresses is equal to the nonequilibrium interface energy, as desired.

For the equilibrium interface, substituting phase equilibrium temperature θ_e, for which

$\Delta G^{\theta}(\theta_e) = 0$ in Eq.(49), we simplify

$$\gamma_e(\boldsymbol{k}, \theta_e) = \frac{\beta(\boldsymbol{k}, \theta_e)\sqrt{2\rho_0 A(\theta_e)}}{6} = \frac{k(\boldsymbol{k}, \theta_e)\beta^2(\boldsymbol{k}, \theta_e)}{6} = \frac{\rho_0 A(\theta_e)}{3k(\boldsymbol{k}, \theta_e)}. \tag{50}$$

The nonequilibrium and equilibrium *interface width* are defined as

$$\delta(\boldsymbol{k}, \theta) := \frac{10}{k(\boldsymbol{k}, \theta)} = \frac{10\beta(\boldsymbol{k}, \theta)}{\sqrt{2B}} = \frac{5}{3}\frac{\beta^2(\boldsymbol{k}, \theta)}{\gamma(\boldsymbol{k}, \theta)}; \quad \delta_e(\boldsymbol{k}, \theta_e) = \frac{10\beta(\boldsymbol{k}, \theta)}{\sqrt{2\rho_0 A(\theta_e)}}. \tag{51}$$

Thus, the orientational dependence of both interface energy and width is proportional to the orientational dependence of the β, which, for cubic crystals, is given in Eq.(40). This differs from relationships in [57] for $\gamma_e(\boldsymbol{k})$ (nonequilibrium interfaces have not been considered in [57]), because it is overlooked that the width of the interface depends on the orientation as well. That is why the ratios

$$\frac{\gamma(\boldsymbol{k}, \theta)}{\delta(\boldsymbol{k}, \theta)} = \frac{\rho_0(A(\theta) - 3\Delta G^{\theta}(\theta))}{30}; \quad \frac{\gamma(\boldsymbol{k}, \theta_e)}{\delta(\boldsymbol{k}, \theta_e)} = \frac{\rho_0 A(\theta_e)}{30} \tag{52}$$

are independent of the interface orientation. Also, temperature-dependence of the product

$$\gamma(\boldsymbol{k}, \theta)\delta(\boldsymbol{k}, \theta) = \frac{5}{3}\beta^2(\boldsymbol{k}, \theta), \tag{53}$$

is independent of $B(\theta)$.

Examples for Na. Function $\gamma(\boldsymbol{k}_0) = \beta(\boldsymbol{k}_0)/Z$ ($Z = 6/\sqrt{2B}$, see Eq.(49)) for Na body centric cubic crystal **in contact with its melt**, for which $\alpha_0 = 0.295$, $\alpha_1 = -0.579$, $\alpha_2 = 1.915$, and $\alpha_3 = 0.477$, all in J/m^2, are taken from [57]), is shown in Fig. 2a. In Fig. 2b, spherical plots of function $\gamma^2(\boldsymbol{k}_0) = \beta^2(\boldsymbol{k}_0)/Z^2 = 2\psi^{\nabla}/(Z^2|\boldsymbol{\zeta}|^2) = \sigma_{st}/(Z^2|\boldsymbol{\zeta}|^2)$ is presented. It is clear that the anisotropy of the biaxial tension is much more pronounced than anisotropy of the interface energy and width. 2D polar plots of these functions for within {110} and {100} planes are shown in Figs. 3 and 4, a and b.

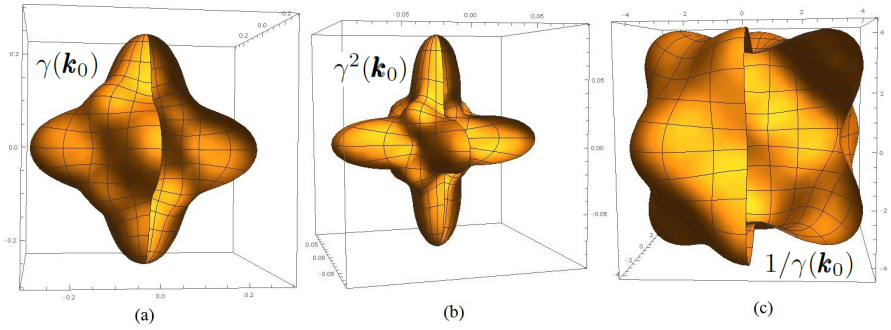

FIG. 2. (a) Orientation dependence of the gradient energy coefficient $\gamma(\boldsymbol{k}_0) = \beta(\boldsymbol{k}_0)/Z$ for Na; interface width $\delta(\boldsymbol{k}_0)$ has the same orientation dependence (Eq.(51)). (b) Spherical plot of the function $\gamma^2(\boldsymbol{k}_0)$, which has same orientation dependence as the magnitude of $\beta^2(\boldsymbol{k}_0)$, the biaxial interface stress $\sigma_{st}(\boldsymbol{k}_0)$, and the gradient energy $\psi^{\nabla}(\boldsymbol{k}_0)$. (c) Orientation dependence of the function $1/\gamma(\boldsymbol{k}_0)$, possessing multiple concave parts that should be regularized with the planes.

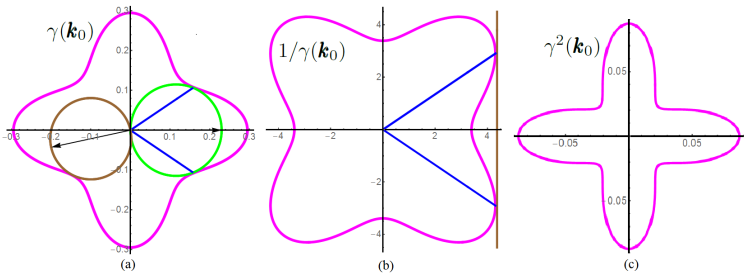

FIG. 3. Polar plots for {110} plane of Na for interface energy $\gamma(\boldsymbol{k}_0)$, which is proportional to the function $\beta(\boldsymbol{k}_0)$ and interface width $\delta(\boldsymbol{k}_0)$ (a), function $1/\gamma(\boldsymbol{k}_0)$ (b), and $\gamma^2(\boldsymbol{k}_0) = \beta^2(\boldsymbol{k}_0)/Z^2 = 2\psi^{\nabla}/(Z^2|\boldsymbol{\zeta}|^2) = \sigma_{st}/(Z^2|\boldsymbol{\zeta}|^2)$ (c). Convexification of a nonconvex part of function $1/\gamma(\boldsymbol{k}_0)$ with the straight line is shown in (b). It corresponds to the substitution of part of the curve $\gamma(\boldsymbol{k}_0)$ in (a), which cannot be touched by a circle $\boldsymbol{g}\cdot\boldsymbol{k}_0$ plotted on the vector $\boldsymbol{g}$ (which is orthogonal to the regularizing line) as on a diameter, without intersecting $\gamma(\boldsymbol{k}_0)$ at other points, with the circle $\gamma_c(\boldsymbol{k}_0) = \boldsymbol{g}\cdot\boldsymbol{k}_0$.

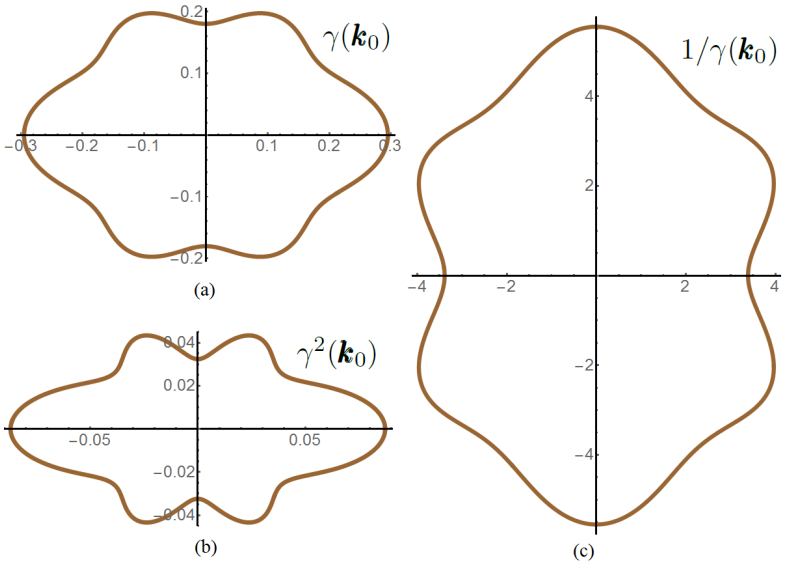

FIG. 4. Polar plots for {100} plane of Na for interface energy function $\gamma(\boldsymbol{k}_0)$, which is similar to the $\beta(\boldsymbol{k}_0)$ and interface width $\delta(\boldsymbol{k}_0)$ (a), function $\gamma^2(\boldsymbol{k}_0) = \beta^2(\boldsymbol{k}_0)/Z^2 = 2\psi^{\nabla}/(Z^2|\boldsymbol{\zeta}|^2) = \sigma_{st}/(Z^2|\boldsymbol{\zeta}|^2)$ (b), and $1/\gamma(\boldsymbol{k}_0)$ (c).

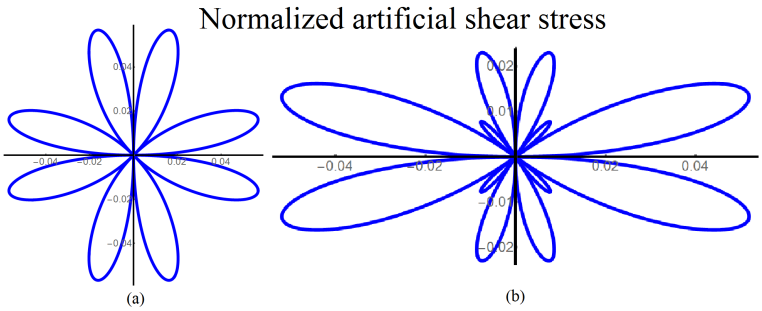

FIG. 5. Polar plots of the artificial shear stresses normalized by $Z^2|\boldsymbol{\zeta}|^2$ for Na for {100} plane (a) and {110} plane (b).

VIII. ARTIFICIAL SHEAR STRESSES AND MOMENTS IN THE PREVIOUS THEORIES

The gradient energy

$$\rho_0\psi^{\nabla} = 0.5\beta^2(\boldsymbol{k})|\boldsymbol{\nabla}\eta|^2 = 0.5\beta^2(\boldsymbol{\zeta}) \tag{54}$$

utilized in the previous theories [9, 10, 13, 37–39, 43], according to equation

$$\boldsymbol{\sigma}_{st} = \rho_0(\breve{\psi}^{\theta} + \psi^{\nabla})\boldsymbol{I} - \rho_0\boldsymbol{\zeta}\otimes\frac{\partial\psi^{\nabla}}{\partial\boldsymbol{\zeta}} \tag{55}$$

(see [35]) leads to the following expression for structural stresses:

$$\boldsymbol{\sigma}^{p}_{st} = (\rho_0\breve{\psi}^{\theta} + 0.5\beta^2(\boldsymbol{k})|\boldsymbol{\zeta}|^2)\boldsymbol{I} - \beta(\boldsymbol{\zeta})\boldsymbol{\zeta}\otimes\frac{\partial\beta(\boldsymbol{\zeta})}{\partial\boldsymbol{\zeta}} = \beta^2(\boldsymbol{\zeta})\left(\boldsymbol{I}-\boldsymbol{k}\otimes\boldsymbol{k}\right) - \boldsymbol{\sigma}^{dif}_{st}, \tag{56}$$

where superscript p is for previous, and

$$\boldsymbol{\sigma}^{dif}_{st} := \beta(\boldsymbol{\zeta})\boldsymbol{\zeta}\otimes\frac{\partial\beta(\boldsymbol{\zeta})}{\partial\boldsymbol{\zeta}} - \beta^2(\boldsymbol{k})\boldsymbol{\zeta}\otimes\boldsymbol{\zeta} \tag{57}$$

is the difference between the previous theory and the correct result in Eq.(47), and the equality (46) is taken into account. In the local Cartesian system of coordinates, in which axis 3 is along the normal $\boldsymbol{k}$ and axes 1 and 2 with unit vectors $\boldsymbol{t}$ and $\boldsymbol{p}$ are within an interface (Fig. 1a), the interface stress $\boldsymbol{\sigma}_{st}$ in our theory represents equal biaxial tension in directions 1 and 2. In evaluating $\boldsymbol{\sigma}^{dif}_{st}$, we recognize that while the term $\beta^2(\boldsymbol{k})\boldsymbol{\zeta}\otimes\boldsymbol{\zeta}$ has the only component 33, the term $\beta(\boldsymbol{\zeta})\boldsymbol{\zeta}\otimes\frac{\partial\beta(\boldsymbol{\zeta})}{\partial\boldsymbol{\zeta}}$ also possesses shear stresses τ_{31} and τ_{32}, which are directed along the axis 3 and act at planes orthogonal to axes 1 and 2). Utilizing Eq.(57) and $\frac{\partial\beta(\boldsymbol{\zeta})}{\partial\boldsymbol{\zeta}}\cdot\boldsymbol{\zeta} = \beta(\boldsymbol{\zeta})$, one has

$$\boldsymbol{\sigma}^{dif}_{st}\cdot\boldsymbol{\zeta} = \beta(\boldsymbol{\zeta})\boldsymbol{\zeta}\frac{\partial\beta(\boldsymbol{\zeta})}{\partial\boldsymbol{\zeta}}\cdot\boldsymbol{\zeta} - \beta^2(\boldsymbol{k})\boldsymbol{\zeta}|\boldsymbol{\zeta}|^2 = \beta^2(\boldsymbol{\zeta})\boldsymbol{\zeta} = \beta^2(\boldsymbol{\zeta})\boldsymbol{\zeta} = \boldsymbol{0}. \tag{58}$$

Consequently, component 33 of $\boldsymbol{\sigma}^{dif}_{st}$ vanishes. Thus, the only non-zero components of $\boldsymbol{\sigma}^{dif}_{st}$ are shear stresses:

$$\tau_{31} = \boldsymbol{k}\cdot\beta(\boldsymbol{\zeta})\boldsymbol{\zeta}\frac{\partial\beta(\boldsymbol{\zeta})}{\partial\boldsymbol{\zeta}}\cdot\boldsymbol{t} = \beta(\boldsymbol{\zeta})|\boldsymbol{\zeta}|\frac{\partial\beta(\boldsymbol{\zeta})}{\partial\boldsymbol{\zeta}}\cdot\boldsymbol{t};\ \tau_{32} = \boldsymbol{k}\cdot\beta(\boldsymbol{\zeta})\boldsymbol{\zeta}\frac{\partial\beta(\boldsymbol{\zeta})}{\partial\boldsymbol{\zeta}}\cdot\boldsymbol{p} = \beta(\boldsymbol{\zeta})|\boldsymbol{\zeta}|\frac{\partial\beta(\boldsymbol{\zeta})}{\partial\boldsymbol{\zeta}}\cdot\boldsymbol{p}, \tag{59}$$

see Fig. 1b. Since $\tau_{13} = \tau_{23} = 0$, according to the angular momentum equation, shear stresses τ_{31} and τ_{32} produce moments about axes 2 and 1, respectively.

The orientation dependence of the normalized biaxial tension for Na is presented in Figs. 2-4. Normalized shear stresses for {110} and {100} planes are shown in Fig. 5. The maximum magnitude of shear stress reaches about 70% of the maximum σ_{st}.

IX. STRONG ANISOTROPY AND CONVEXIFICATION OF $\beta(\zeta)$

Plots of $1/\gamma(\boldsymbol{k}_0) = Z/\beta(\boldsymbol{k}_0)$ are included in Figs. 2-4 because if they are concave, the Ginzburg-Landau equation is ill-posed and orientations with high interface energy are not present in the equilibrium microstructure [38, 59, 60]. For regularization of the problem [38, 59, 60], the nonconvex regions of $1/\gamma(\boldsymbol{k}_0)$ are substituted with the common tangent plane $\frac{1}{\gamma_c(\boldsymbol{k}_0)} = \frac{A}{\boldsymbol{s}\cdot\boldsymbol{k}_0}$, where $\boldsymbol{s}$ is the unit normal to the plane and A is the distance to the plane from the origin (Fig. 3b). The corresponding function $\gamma_c(\boldsymbol{k}_0) = \bar{\boldsymbol{g}} \cdot \boldsymbol{k}_0$ ($\bar{\boldsymbol{g}} := \boldsymbol{s}/A$) represents a sphere plotted on the vector $\bar{\boldsymbol{g}}$ as on the diameter (Fig. 3a). It substitutes $\gamma(\boldsymbol{k}_0)$ for those directions $\boldsymbol{k}_0$, for which it cannot touch $\gamma(\boldsymbol{k}_0)$ without intersecting $\gamma(\boldsymbol{k}_0)$ at other points. All points in convex regions of $1/\gamma(\boldsymbol{k}_0)$ can be touched by a sphere $\boldsymbol{B} \cdot \boldsymbol{k}_0$ for some vector-diameter $\boldsymbol{B}$ (Fig. 3a). For such a $\gamma_c(\boldsymbol{k}_0) = \bar{\boldsymbol{g}} \cdot \boldsymbol{k}_0$ and corresponding $\beta_c(\boldsymbol{k}_0) = \boldsymbol{g} \cdot \boldsymbol{k}_0$ with $\boldsymbol{g} = Z\bar{\boldsymbol{g}}$, all equations become simpler:

$$\beta_c(\boldsymbol{\zeta}_0) = \boldsymbol{g} \cdot \boldsymbol{\zeta}_0 = |\boldsymbol{g}||\boldsymbol{\zeta}_0| \cos\vartheta; \quad \frac{\partial \beta_c}{\partial \boldsymbol{\zeta}_0} = \boldsymbol{g}; \quad \frac{\partial^2 \beta_c}{\partial \boldsymbol{\zeta}_0 \partial \boldsymbol{\zeta}_0} = \boldsymbol{0}. \tag{60}$$

Here ϑ is the angle between the vectors $\boldsymbol{g}$ and $\boldsymbol{\zeta}_0$. Then for coplanar vectors $\boldsymbol{t}$, $\boldsymbol{g}$, and $\boldsymbol{\zeta}_0$ we obtain

$$\begin{aligned} &\tau_{31} = \beta_c(\boldsymbol{\zeta}_0)|\boldsymbol{\zeta}_0|\boldsymbol{g} \cdot \boldsymbol{t} = |\boldsymbol{g}||\boldsymbol{\zeta}_0|^2 \cos\vartheta |\boldsymbol{g}| \cos(\pi/2 + \vartheta) = -0.5|\boldsymbol{g}|^2|\boldsymbol{\zeta}_0|^2 \sin 2\vartheta; \\ &\sigma_{st} = \beta_c(\boldsymbol{\zeta}_0)^2 = |\boldsymbol{g}|^2|\boldsymbol{\zeta}_0|^2 \cos^2\vartheta; \quad \frac{|\tau_{31}|}{\sigma_{st}} = \tan\vartheta. \end{aligned} \tag{61}$$

The ratio $|\tau_{31}|/\sigma_{st}$ is a growing function ϑ. Maximum ϑ is determined by the points in which the sphere $\gamma_c(\boldsymbol{k}_0) = \bar{\boldsymbol{g}} \cdot \boldsymbol{k}_0 = |\boldsymbol{g}| \cos\vartheta$ and $\gamma(\boldsymbol{k}_0)$ touch. The touching is described by equations

$|\bar{\boldsymbol{g}}|\cos\vartheta = \gamma(\boldsymbol{k}_0)$ and $d|\bar{\boldsymbol{g}}|\cos\vartheta = d\gamma(\boldsymbol{k}_0)$. For a 2D case and horizontal $\bar{\boldsymbol{g}}$ (Fig. 3a), we obtain $\tan\vartheta = -\frac{1}{\gamma}\frac{d\gamma}{d\vartheta}$. For Na $\vartheta_{max} = 0.593$ and $\tan\vartheta_{max} = 0.674$ for $\{100\}$ plane and $\vartheta_{max} = 0.477$ and $\tan\vartheta_{max} = 0.517$ for $\{110\}$ plane.

X. RESULTS FOR A SPECIFIC MODEL

We will perform the same specification as in [33] but for $\beta(\theta)$ substituted with $\beta^2(\boldsymbol{k},\theta)$ (since here we use the expression for the gradient energy typical for papers on anisotropic interface energy, i.e., with β^2 instead of β) and k substituted with $k(\boldsymbol{k},\theta)$. That is why we will focus on the final equations since the derivations are very similar to those in [33].

Energy and entropy excess. It is routinely accepted [33]

$$A = A_0\,(\theta - \theta_c)\ ,\ A_0 > 0; \qquad \Delta G^{\theta}(\theta) = -\Delta s_0(\theta - \theta_e)\ ,\ \Delta s_0 < 0, \tag{62}$$

where θ_c is the critical temperature at which H loses its thermodynamic stability and Δs_0 is the jump in entropy between L and H. Below we utilize the dimensionless temperature, $\bar{\theta}$, and other parameters:

$$\bar{\theta} := \frac{\theta - \theta_e}{\theta_e - \theta_c}; \quad \varpi := -\frac{3\Delta s_0}{A_0} > 0.5; \quad \Upsilon := \bar{\theta}(1-\varpi) + 1 \geq 0; \quad \tilde{A} := 2\rho_0 A_0(\theta_e - \theta_c). \tag{63}$$

The interface energy in Eq.(49) is expressed as

$$\gamma = \frac{\beta(\boldsymbol{k},\theta)\sqrt{2\rho_0 A_0(\theta_e - \theta_c)}}{6}\sqrt{\bar{\theta}(1-\varpi)+1} = \frac{\beta(\boldsymbol{k},\theta)\sqrt{\tilde{A}\Upsilon}}{6}; \quad \gamma_e = \frac{\beta(\boldsymbol{k},\theta)\sqrt{\tilde{A}}}{6}. \tag{64}$$

Excess of an interface entropy is evaluated as:

$$s_i = -\frac{\partial\gamma}{\partial\theta} = \frac{\beta(\boldsymbol{k},\theta)\sqrt{2\rho_0 A_0}}{12\sqrt{\theta_e - \theta_c}}\frac{\varpi - 1}{\sqrt{\bar{\theta}(1-\varpi)+1}} + \frac{\partial\beta(\boldsymbol{k},\theta)}{\partial\theta}\frac{\sqrt{\tilde{A}\Upsilon}}{6}. \tag{65}$$

Interface width. Parameter k can be expressed with the help of Eqs.(44) or (49):

$$k(\boldsymbol{k},\theta) = \frac{\sqrt{\tilde{A}[\bar{\theta}(1-\varpi)+1]}}{\beta(\boldsymbol{k},\theta)} = \frac{6\gamma(\boldsymbol{k},\theta)}{\beta^2(\boldsymbol{k},\theta)}. \tag{66}$$

Then the interface width at temperature θ and θ_e is:

$$\delta(\boldsymbol{k},\theta) := \frac{10}{k(\boldsymbol{k},\theta)} = \frac{10\beta(\boldsymbol{k},\theta)}{\sqrt{\tilde{A}[\bar{\theta}(1-\varpi)+1]}} = \frac{5\beta^2(\boldsymbol{k},\theta)}{3\gamma(\boldsymbol{k},\theta)}; \quad \delta(\theta_e) = 10\frac{\beta(\boldsymbol{k},\theta_e)}{\sqrt{\tilde{A}}}. \tag{67}$$

Let us define $\beta_0(\theta)$ and the interface width $\delta_0(\theta)$ in the direction $< 100 >$. Below we will use the dimensionless interface width $\tilde{\delta}$ normalized by the interface width $\delta_0(\theta_e)$:

$$\tilde{\delta} := \frac{\delta(\boldsymbol{k},\theta)}{\delta_0(\theta_e)} = \frac{\beta(\boldsymbol{k},\theta)}{\beta_0(\theta)\sqrt{[\bar{\theta}(1-\varpi)+1]}}. \tag{68}$$

Interface stress. The magnitude of the biaxial interface stress is:

$$\sigma_{st} = 2\rho_0\breve{\psi}^{\theta} = 2\rho_0 A_0[(\theta-\theta_e)(1-\varpi)+(\theta_e-\theta_c)]\eta_{in}^2(1-\eta_{in})^2 = \tilde{A}\Upsilon\eta_{in}^2(1-\eta_{in})^2. \tag{69}$$

Since the interface profile is the same for any t, we can consider $t = 0$ without loss of generality. It is convenient to transform

$$e^{-\zeta} = e^{-k(\boldsymbol{k},\theta)x} = e^{-10x/\delta(\boldsymbol{k},\theta)} = e^{-\frac{10x}{\delta_0(\theta_e)}\frac{\delta_0(\theta_e)}{\delta((\boldsymbol{k},\theta))}} = e^{-10y/\tilde{\delta}(\boldsymbol{k},\theta)}; \quad y := \frac{x}{\delta_0(\theta_e)}, \tag{70}$$

where the factor of 10 is an approximate width of the interface $\eta_{in}(\zeta)$ and the dimensionless coordinate y is introduced in which the interface width $\simeq 1$ at $\theta = \theta_e$ in $< 100 >$ direction. Then Eqs.(44) and (69) result in the distribution of the magnitude of the interface stresses and their dimensionless analog $\bar{\sigma}_{st}$:

$$\sigma_{st} = \tilde{A}\Upsilon\frac{e^{-20y/\tilde{\delta}(\boldsymbol{k},\theta)}}{\left(1+e^{-10y/\tilde{\delta}(\boldsymbol{k},\theta)}\right)^4} \qquad \bar{\sigma}_{st} := \frac{\sigma_{st}}{\tilde{A}\Upsilon} = \frac{e^{-20y/\tilde{\delta}(\boldsymbol{k},\theta)}}{\left(1+e^{-10y/\tilde{\delta}(\boldsymbol{k},\theta)}\right)^4}. \tag{71}$$

The maximum dimensionless surface stress is independent of direction $\boldsymbol{k}$ and is $1/16$ at $y = 0$. A plot of $\bar{\sigma}_{st}(y)$ for $\theta = \theta_e$ and several directions $\boldsymbol{k}$ is shown in Fig. 6 for fcc Al and bcc Na. The area below the plots is proportional to the interface energy $\gamma(\boldsymbol{k},\theta_e)$, which has the same $\boldsymbol{k}$-dependence as $\tilde{\delta}$ and β. Different crystallographic directions for maximum and minimum width of the interface for Al and Na exhibits different types of anisotropy for these crystals.

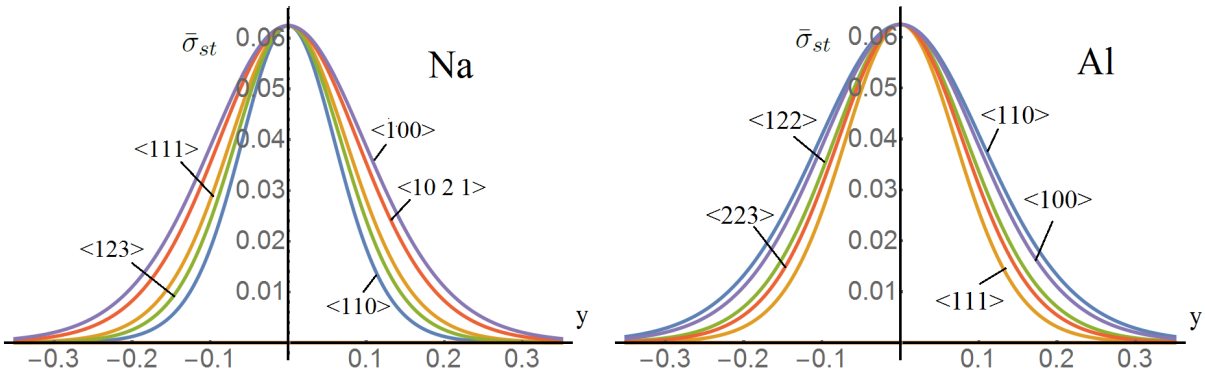

FIG. 6. Distribution of the dimensionless biaxial surface tension $\bar{\sigma}_{st}(y)$ for an equilibrium interface for several directions $\boldsymbol{k}$ for bcc Na and fcc Al.

XI. INTERFACE STRESSES FOR CRITICAL NUCLEUS

All results for a critical nucleus in [33] are valid here provided we add the $\boldsymbol{k}$-dependence of β and width of the critical nucleus l. Thus, the stationary solution of the Ginzburg-Landau equation for the critical nucleus

$$\eta_c = 6\left[6 - P + \sqrt{P^2 - 3P}\, cosh\left(20\sqrt{\bar{\theta}+1}\, y/\tilde{l}(\boldsymbol{k},\theta)\right)\right]^{-1}; \quad P := 4\varpi\bar{\theta}/(\bar{\theta}+1);$$
$$l(\boldsymbol{k},\theta) := 10\sqrt{2}\beta(\boldsymbol{k},\theta)/\sqrt{\tilde{A}}; \quad y := x/l((1,0,0),\theta); \quad \tilde{l}(\boldsymbol{k},\theta) := l(\boldsymbol{k},\theta)/l((1,0,0),\theta) \quad (72)$$

is expressed in terms of a more convenient dimensionless coordinate y. It is plotted in Fig. 7 for Na for $\varpi = 1$, $\bar{\theta} = -0.01$, and three crystallographic directions. For each point of the nucleus

$$\psi^{\nabla}(\boldsymbol{k},\theta,\eta_c) = \breve{\psi}^{\theta}(\theta,\eta_c) + \tilde{\psi}^{\theta}(\theta,\eta_c); \quad \psi(\boldsymbol{k},\theta,\eta_c) = \psi^{\nabla}(\boldsymbol{k},\theta,\eta_c) + \breve{\psi}^{\theta}(\theta,\eta_c) + \tilde{\psi}^{\theta}(\theta,\eta_c)$$
$$= 2\psi^{\nabla}(\boldsymbol{k},\theta,\eta_c) = 2(\breve{\psi}^{\theta}(\theta,\eta_c) + \tilde{\psi}^{\theta}(\theta,\eta_c)). \quad (73)$$

Substituting Eq.(73) into Eq.(35) for the interface stresses, one obtains

$$\boldsymbol{\sigma}_{st} = \rho_0\psi(\boldsymbol{k},\theta,\eta_c)\,(\boldsymbol{I} - \boldsymbol{k}\otimes\boldsymbol{k}) - \rho_0\tilde{\psi}^{\theta}(\theta,\eta_c)\boldsymbol{I}. \quad (74)$$

Thus, the magnitude of the tensile biaxial interface stress is equal at each point to the local total free energy per unit volume $\rho_0\psi(\boldsymbol{k},\theta,\eta_c)$. Consequently, the total interface force is also equal to the total free energy of a critical nucleus. In addition, the tensile mean stress $-\rho_0\tilde{\psi}^\theta > 0$ is acting at each point of a nucleus. It is also orientation-dependent because of the orientation dependence of the solution η_c.

The dimensionless magnitude of the biaxial surface stress $\tilde{\sigma}_{st}(y) := \frac{\psi(\theta,\eta_c)}{A_0(\theta_e-\theta_c)}$ and dimensionless mean stress $p(y) := -\frac{\tilde{\psi}^\theta(\theta,\eta_c)}{A_0(\theta_e-\theta_c)}$ are shown in Fig. 7 for three crystal orientations. One can see that the surface tension is concentrated at the incomplete interfaces and is negligible at the center of a nucleus. Since the driving force for transformation is relatively small, the maximum value of η_c is close to unity and the structure of the nucleus is close to two almost complete separated interfaces. That is why the magnitude of a biaxial tension is close to that in Fig. 6 and tensile mean stress is smaller by a factor of 20. The area below the $\tilde{\sigma}_{st}(x/l)$ curve represents total force and, consequently, the energy of the critical nucleus normalized by $A_0(\theta_e-\theta_c)$. All fields in Fig. 7 depend on orientation through the width of a nucleus and the maximum of all fields is orientation-independent.

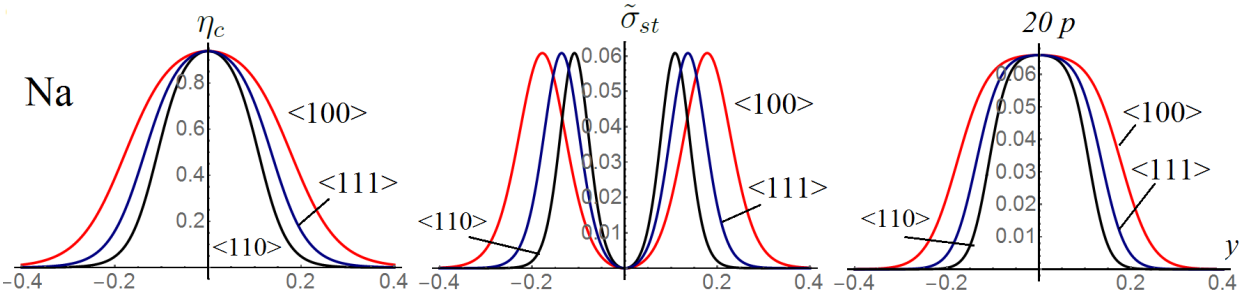

FIG. 7. Profile of the critical nucleus $\eta_c(y)$, and distribution of the dimensionless biaxial surface tension $\tilde{\sigma}_{st}$ and dimensionless mean stress p for three different orientations of Na crystal for $\varpi = 1$ and $\bar{\theta} = -0.01$.

XII. CONCLUDING REMARKS

In this work we generalized a PFA developed in [33] for anisotropic interface energy and stresses. Previous papers on this topic overlooked that the nonsymmetric stress tensor, which is the consequence of anisotropic dependence of the gradient energy on $\boldsymbol{\nabla}\eta_i$, violates the angular momentum balance and principle of material objectivity. In the new theory developed here, this problem was overcome by assuming that the gradient energy is an *isotropic* function of the gradient of the order parameters in the *current* state, which also depends on the direction of the gradient of the order parameters in the *reference* state. Thus, some elements of finite strain formulation should be included in the current small strain theory. This leads to a symmetric stress tensor that transforms to the biaxial tension with the magnitude equal to the orientation- and temperature-dependent interface energy for the nonequilibrium interface. The new Ginzburg-Landau equations have many extra terms due to anisotropy of the interface energy. They are all of the first order of smallness for small strains which is, surprisingly, a more important strain-related contribution than the next significant term which comes from mechanics. Indeed, the largest mechanical contribution, which is the transformation work, is cubic in small strains. The analytical study of the propagating interface and critical nucleus is not much more complicated than for an isotropic interface: one just has to substitute gradient energy and the kinetic coefficient with their orientational dependence. The analytical relationship for such dependence for the gradient energy coefficient is obtained in [57] using molecular dynamics.

The developed PFA is applicable to melting or solidification [9–14, 30, 43], sublimation, amorphization, and can be generalized for solid-solid PTs [1–6, 8, 32, 61], twinning [15, 16], grain growth [17], fracture [54, 62], and interaction of cracks and dislocations with PTs [63–72], for which the interface energy depends on interface orientation of crystals from both its sides. It also has to be generalized for fully large strain formulation [35] and multivariant martensitic transformations and multiphase materials [73].

Similarly orientation-dependence can be introduced in the expression for energy of the external surface for a sharp [14, 32, 74] and finite-width [55, 75] treatment of the external surfaces. It may lead to reshaping and faceting of nanowires [76] and other nanoobjects. It also can be included for melting within grain boundaries [77] and at the interfaces between two solid phases [76, 78–81]. Note that reorientation of an interface may occur due to applied stresses and corresponding thermodynamic driving force is found in [82, 83]. In PFA, such a reorientation will occur automatically.

Acknowledgement

The support of NIST, NSF (CMMI-1536925 and DMR-1434613), ARO (W911NF-12-1-0340), DARPA (W31P4Q-13-1-0010), ONR, and Iowa State University are gratefully acknowledged. A major part of this work was performed during VIL sabbatical stay at NIST. Certain commercial software and materials are identified in this report in order to specify the procedures adequately. Such identification is not intended to imply recommendation or endorsement by the National Institute of Standards and Technology, nor is it intended to imply that the materials or software identified are necessarily the best available for the purpose.

Appendix

Below, the derivatives of all β-related terms in Eqs.(36) and (26) are presented in the component form:

$$\frac{\partial\beta}{\partial\zeta_{0i}} = \alpha_0\frac{\zeta_{0i}}{|\boldsymbol{\zeta}_0|} + \alpha_1\left(2\frac{\zeta_{0i}\left(\zeta_{0j}^2+\zeta_{0k}^2\right)}{|\boldsymbol{\zeta}_0|^3} - 3\frac{\zeta_{0i}\left(\zeta_{0i}^2\zeta_{0j}^2+\zeta_{0i}^2\zeta_{0k}^2+\zeta_{0k}^2\zeta_{0j}^2\right)}{|\boldsymbol{\zeta}_0|^5}\right) + \alpha_2\left(\frac{2\zeta_{0i}\zeta_{0j}^2\zeta_{0k}^2}{|\boldsymbol{\zeta}_0|^5} - \frac{5\zeta_{0i}^3\zeta_{0j}^2\zeta_{0k}^2}{|\boldsymbol{\zeta}_0|^7}\right) + \alpha_3\left(\frac{4\zeta_{0i}\left(\zeta_{0j}^2+\zeta_{0k}^2\right)\left(\zeta_{0i}^2\zeta_{0j}^2+\zeta_{0i}^2\zeta_{0k}^2+\zeta_{0k}^2\zeta_{0j}^2\right)}{|\boldsymbol{\zeta}_0|^7} - \frac{7\zeta_{0i}\left(\zeta_{0i}^2\zeta_{0j}^2+\zeta_{0i}^2\zeta_{0k}^2+\zeta_{0k}^2\zeta_{0j}^2\right)^2}{|\boldsymbol{\zeta}_0|^9}\right); \quad (75)$$

$$\frac{\partial^2\beta}{\partial\zeta_{0i}\partial\zeta_{0k}} = -\alpha_0\frac{\zeta_{0i}\zeta_{0k}}{|\boldsymbol{\zeta}_0|^3} - \alpha_1\left(\frac{2\zeta_{0i}\zeta_{0k}\left(\zeta_{0i}^2+\zeta_{0k}^2+4\zeta_{0j}^2\right)}{|\boldsymbol{\zeta}_0|^5} - \frac{15\zeta_{0i}\zeta_{0k}\left(\zeta_{0i}^2\zeta_{0j}^2+\zeta_{0i}^2\zeta_{0k}^2+\zeta_{0k}^2\zeta_{0j}^2\right)}{|\boldsymbol{\zeta}_0|^7}\right)$$
$$-\alpha_2\frac{\zeta_{0i}\zeta_{0j}^2\zeta_{0k}\left(6\zeta_{0i}^4-4\zeta_{0j}^4+6\zeta_{0k}^4+2\zeta_{0j}^2\zeta_{0k}^2+2\zeta_{0i}^2\zeta_{0j}^2-23\zeta_{0i}^2\zeta_{0k}^2\right)}{|\boldsymbol{\zeta}_0|^9} +$$
$$\alpha_3\left(\frac{8\zeta_{0i}\zeta_{0k}\left(\zeta_{0j}^4+2\zeta_{0j}^2\zeta_{0k}^2+2\zeta_{0i}^2\left(\zeta_{0k}^2+\zeta_{0j}^2\right)\right)}{|\boldsymbol{\zeta}_0|^7} + \frac{63\zeta_{0i}\zeta_{0k}\left(\zeta_{0i}^2\zeta_{0j}^2+\zeta_{0i}^2\zeta_{0k}^2+\zeta_{0k}^2\zeta_{0j}^2\right)^2}{|\boldsymbol{\zeta}_0|^{11}} -\right.$$
$$\left.\frac{28\zeta_{0i}\zeta_{0k}\left(\zeta_{0i}^4\left(\zeta_{0k}^2+\zeta_{0j}^2\right)+\zeta_{0k}^2\zeta_{0j}^2\left(\zeta_{0k}^2+2\zeta_{0j}^2\right)+\zeta_{0i}^2\left(2\zeta_{0j}^4+4\zeta_{0j}^2\zeta_{0k}^2+\zeta_{0k}^4\right)\right)}{|\boldsymbol{\zeta}_0|^9}\right), \tag{76}$$

and

$$\frac{\partial^2\beta}{\partial\zeta_{0i}^2} = \alpha_0\left(\frac{1}{|\boldsymbol{\zeta}_0|} - \frac{\zeta_{0i}^2}{|\boldsymbol{\zeta}_0|^3}\right) + \alpha_1\left(\frac{2\left(\zeta_{0j}^2+\zeta_{0k}^2\right)}{|\boldsymbol{\zeta}_0|^3} - \frac{3\left(3\zeta_{0i}^2\zeta_{0j}^2+3\zeta_{0i}^2\zeta_{0k}^2-\zeta_{0k}^2\zeta_{0j}^2\right)}{|\boldsymbol{\zeta}_0|^5} +\right.$$
$$\left.\frac{15\zeta_{0i}^2\left(\zeta_{0i}^2\zeta_{0j}^2+\zeta_{0i}^2\zeta_{0k}^2+\zeta_{0k}^2\zeta_{0j}^2\right)}{|\boldsymbol{\zeta}_0|^7}\right) + \alpha_2\frac{\zeta_{0j}^2\zeta_{0k}^2\left(12\zeta_{0i}^4-21\zeta_{0i}^2\left(\zeta_{0j}^2+\zeta_{0k}^2\right)+2\left(\zeta_{0j}^2+\zeta_{0k}^2\right)^2\right)}{|\boldsymbol{\zeta}_0|^9} +$$
$$\alpha_3\left(\frac{4\left(\zeta_{0k}^2+\zeta_{0j}^2\right)\left(\zeta_{0j}^2\zeta_{0k}^2+3\zeta_{0i}^2\left(\zeta_{0k}^2+\zeta_{0j}^2\right)\right)}{|\boldsymbol{\zeta}_0|^7} + \frac{63\zeta_{0i}^2\left(\zeta_{0i}^2\zeta_{0j}^2+\zeta_{0i}^2\zeta_{0k}^2+\zeta_{0k}^2\zeta_{0j}^2\right)^2}{|\boldsymbol{\zeta}_0|^{11}} -\right.$$
$$\left.\frac{7\left(\zeta_{0j}^4\zeta_{0k}^4+10\zeta_{0i}^2\zeta_{0j}^2\zeta_{0k}^2\left(\zeta_{0k}^2+\zeta_{0j}^2\right)+9\zeta_{0i}^4\left(\zeta_{0k}^2+\zeta_{0j}^2\right)^2\right)}{|\boldsymbol{\zeta}_0|^9}\right). \tag{77}$$

For a two-dimensional case one has to put $\zeta_{0j}=0$; the terms with α_2 in this case disappears.

---

[1] Y.M. Jin, A. Artemev, and A.G. Khachaturyan, Three-Dimensional Phase Field Model of Low-Symmetry Martensitic Transformation in Polycrystal: Simulation of ζ_2 Martensite in AuCd Alloys, Acta Mat. 49, 2309 (2001).

[2] L.Q. Chen, Phase-Field Models for Microstructure Evolution, Annu. Rev. Mater. Res. 32, 113 (2002).

[3] T. Lookman, A. Saxena, and R.C. Albers, Phonon Mechanisms and Transformation Paths in Pu, Phys. Rev. Lett. 100, 145504 (2008).

[4] V.I. Levitas and D.W. Lee, Athermal Resistance to an Interface Motion in Phase Field Theory of Microstructure Evolution, Phys. Rev. Lett. 99, 245701 (2007).

[5] V.I. Levitas, A.V. Idesman, and D.L. Preston, Microscale Simulation of Evolution of Martensitic Microstructure, Phys. Rev. Lett. 93, 105701 (2004).

[6] A. Artemev, Y. Jin, and A.G. Khachaturyan, Three-Dimensional Phase Field Model of Proper Martensitic Transformation, Acta Mater. 49, 1165 (2001).

[7] J. Svoboda, F.D. Fischer, and D.L. McDowell, Derivation of the Phase Field Equations from the Thermodynamic Extremal Principle, Acta Mater. 60, 396 (2012).

[8] A. Finel, Y. Le Bouar, A. Gaubert, and U. Salman, Phase Field Methods: Microstructures, Mechanical Properties, and Complexity, C. R. Physique 11, 245 (2010).

[9] R. Kobayashi, Modeling and Numerical Simulations of Dendritic Crystal Growth, Physica D 63, 410 (1993).

[10] D.M. Anderson, G.B. McFadden, and A.A. Wheeller, A Phase-Field Model of Solidification with Convection, Physica D 135, 175 (2000).

[11] D.M. Anderson, G.B. McFadden, and A.A. Wheeller, A Phase-Field Model with Convection: Sharp-Interface Asymptotics, Physica D 151, 305 (2001).

[12] J. Slutsker, K. Thornton, A.L. Roytburd, J.A. Warren, and G.B. McFadden, Phase Field Modeling of Solidification Under Stress, Phys. Rev. B 74, 014103 (2006).

[13] J.A. Warren and W.J. Boettinger, Prediction of Dendritic Growth and Microsegregation Patterns in a Binary Alloy Using the Phase-Field Method, Acta Mater. 43, 689 (1995).

[14] V.I. Levitas and K. Samani, Size and Mechanics Effects in Surface-Induced Melting of Nanoparticles, Nat. Commun. 2, 284 (2011).

[15] J.D. Clayton and J. Knap, A Phase Field Model of Deformation Twinning: Nonlinear Theory and Numerical Simulations, Physica D 240, 841 (2011).

[16] V.I. Levitas, A.M. Roy, and D.L. Preston, Multiple Twinning and Variant-Variant Transformations in Martensite: Phase-Field Approach, Phys. Rev. B 88, 054113 (2013).

[17] R. Kobayashi, J.A. Warren, and W.C. Carter, Vector-Valued Phase Field Model for Crystal-

lization and Grain Boundary Formation, Physica D 140, 141 (1998).

[18] L. E. Malvern, Introduction to the Mechanics of a Continuous Medium (Prentice Hall, NY, 1977).

[19] J.W. Gibbs, The Collected Works of J. Willard Gibbs (Yale University Press, New Haven, 1948).

[20] R. Shuttleworth, The surface tension of solids. Proc. Phys. Soc. A, 63, 444 (1950).

[21] J.W. Cahn, Theromodynamics of Solid and Fluid Surfaces. In Interface Segregation, edited by W.C. Johnson and J.M. Blackely, American Society of Metals, Chap. 1, p.3.

[22] M.E. Gurtin and A. Struthers, Multiphase Thermomechanics with Interfacial Structure 3. Evolving Phase Boundaries in the Presence of Bulk Deformation, Arch. Rat. Mech. Anal. 112, 97 (1990).

[23] Ya.S. Podstrigach and Yu.Z. Povstenko, Introduction in Mechanics of Surface Phenomena in Deformable Solids, Kiev: Naukova Dumka (1985).

[24] M.E. Gurtin and A. Murdoch, A Continuum Theory of Elastic Material Surfaces, Arch. Rat. Mech. Anal. 57, 291 (1975).

[25] A. Javili and P. Steinmann, On Thermomechanical Solids with Boundary Structures, Int. J. Solids Struct. 47, 3245 (2010).

[26] H.L. Duan, J. Wang, and B.L. Karihaloo, Theory of Elasticity at the Nanoscale, Adv. Appl. Mech. 42, 1 (2009).

[27] F.D. Fischer, T. Waitz, D. Vollath, and N.K. Simha, On the Role of Surface Energy and Surface Stress in Phase-Transforming Nanoparticles, Prog. Mat. Sci. 53, 481 (2008).

[28] T. Frolov and Y. Mishin, Orientation Dependence of the Solid-Liquid Interface Stress: Atomistic Calculations for Copper, Modelling Simul. Mater. Sci. Eng. 18, 074003 (2010).

[29] T. Frolov and Y. Mishin, Effect of Nonhydrostatic Stresses on Solid-Fluid Equilibrium. II. Interface Thermodynamics, Phys. Rev. B 82, 174114 (2010).

[30] V.I. Levitas and K. Samani, Coherent Solid-Liquid Interface with Stress Relaxation in a Phase-Field Approach to the Melting/Freezing Transition, Phys. Rev. B 84, 140103 (2011).

[31] E. Fried and G. Grach, An Order-Parameter-Based Theory as a Regularization of a Sharp-Interface Theory for Solid-Solid Phase Transitions, Arch. Rat. Mech. Anal. 138,355 (1997).

[32] V.I. Levitas and M. Javanbakht, Surface Tension and Energy in Multivariant Martensitic Transformations: Phase-Field Theory, Simulations, and Model of Coherent Interface, Phys. Rev. Lett. 105, 165701 (2010).

[33] V.I. Levitas, Thermodynamically Consistent Phase Field Approach to Phase Transformations with Interface Stresses, Acta Mater. 61, 4305 (2013).

[34] V.I. Levitas, Interface Stress for Nonequilibrium Microstructures in the Phase Field Approach: Exact Analytical Results, Phys. Rev. B 87, 054112 (2013).

[35] V.I. Levitas, Phase Field Approach to Martensitic Phase Transformations with Large Strains and Interface Stresses, J. Mech. Phys. Solids 70, 154 (2014).

[36] V.I. Levitas, Unambiguous Gibbs Dividing Surface for Nonequilibrium Finite-Width Interface: Static Equivalence Approach, Phys. Rev. B 89, 094107 (2014).

[37] A.A. Wheeler and G.B. McFadden, On the Notion of a ξ-Vector and a Stress Tensor for a General Class of Anisotropic Diffuse Interface Models, Proc. R. Soc. London A 453, 1611 (1997).

[38] J.E. Taylor and J.W. Cahn, Diffuse Interfaces with Sharp Corners and Facets: Phase Field Models with Anisotropic Surfaces, Physica D 112, 381 (1998).

[39] J.E. Taylor and J.W. Cahn, Linking Anisotropic Sharp and Diffuse Surface Motion Laws by Gradient Flows, J. Stat. Phys. 77, 183 (1994).

[40] D.W. Hoffman and J.W. Cahn, A Vector Thermodynamics for Anisotropic Surfaces. I. Fundamentals and Application to Plane Surface Junctions, Surf. Sci. 31, 368 (1972).

[41] J.W. Cahn and D.W. Hoffman, A Vector Thermodynamics for Anisotropic Surfaces. II. Curved and Faceted Surfaces, Acta Metall. Mater. 22, 1205 (1974).

[42] R.J. Braun, J.W. Cahn, G.B. McFadden, and A.A. Wheeler, Anisotropy of Interfaces in an Ordered Alloy: a Multiple-Order-Parameter Model, Phil. Trans. R. Soc. Lond. A 355, 1787 (1997).

[43] J.M. Debierre, A. Karma, F. Celestini, and R. Guerin, Phase-Field Approach for Faceted Solidification. Phys. Rev. E 68, 041604 (2003).

[44] J.D. Eshelby, The Force on an Elastic Singularity, Phil. Trans. Roy. Soc. A 244, 87 (1951).

[45] J.D. Eshelby, Energy Relations and the Energy-Momentum Tensor in Continuum Mechanics, *Inelastic Behaviour of Solids*, eds M.F. Kanninen *et al.* (McGraw Hill, New York 1970), p. 77.

[46] G.A. Maugin, Material Inhomogeneities in Elasticity (Chapman and Hall, London, 1993).

[47] M.E. Gurtin, Configurational Force as a Basic Concept of Continuum Physics (Springer-Verlag, New York, 2000).

[48] C. Herring, Surface Tension as a Motivation for Sintering. In The Physics of Powder Metallurgy (McGraw Hill, New York, 1951), p. 143.

[49] R.D. Mindlin, Microstructure in Linear Elasticity, Archive of Rational Mechanics and Analysis 16, 51 (1964).

[50] A.C. Eringen and C.B. Kafadar, Polar field theories. In: Eringen, A.C. (Ed.), Continuum Physics (Academic Press, New York, 1976), Vol. IV, p. 1.

[51] V.I. Levitas, V.A. Levin, K.M. Zingerman, E.I. Freiman, Displacive phase transitions at large strains: Phase-field theory and simulations. Phys. Rev. Lett. 103, 025702 (2009).

[52] F.E. Hildebrand, C. Miehe, A phase field model for the formation and evolution of martensitic laminate microstructure at finite strains. Phil. Mag. 92, 1-41 (2012).

[53] V.I. Levitas, Phase-field theory for martensitic phase transformations at large strains. Int. J. Plasticity 49, 85-118 (2013).

[54] J.D. Clayton and J. Knap, A geometrically nonlinear phase field theory of brittle fracture. Int. J. Fracture 189, 139-148 (2014).

[55] V.I. Levitas and M. Javanbakht, Surface-Induced Phase Transformations: Multiple Scale and Mechanics Effects and Morphological Transitions, Phys. Rev. Lett. 107, 175701 (2011).

[56] V.I. Levitas and K. Samani, Melting and Solidification of Nanoparticles: Scale Effects, Thermally Activated Surface Nucleation, and Bistable States. Phys. Rev. B 89, 075427 (2014).

[57] R.S. Qin and H.K.D.H Bhadeshia, Phase-Field Model Study of the Effect of Interface

Anisotropy on the Crystal Morphological Evolution of Cubic Metals. Acta Mater. 57, 2210 (2009).

[58] V.I. Levitas, D.W. Lee, and D.L. Preston, Interface Propagation and Microstructure Evolution in Phase Field models of Stress-Induced Martensitic Phase Transformations, Int. J. Plasticity 26, 395 (2010).

[59] H.K. Lin, C.C. Chen, and C.W. Lan, Adaptive Three-Dimensional Phase-Field Modeling of Dendritic Crystal Growth with High Anisotropy, J. Cryst. Growth 318, 51 (2011).

[60] J.J. Eggleston, G.B. McFadden, and P.W. Voorhees, A Phase-Field Model for Highly Anisotropic Interfacial Energy, Physica D 150, 91 (2001).

[61] S. Vedantam and R. Abeyaratne, A Helmholtz Free-Energy Function for a Cu-Al-Ni Shape Memory Alloy, Int. J. Non-Linear Mechanics 40, 177 (2005).

[62] Y.M. Jin, Y.U. Wang, and A.G. Khachaturyan, Three-Dimensional Phase Field Microelasticity Theory and Modelling of Multiple Cracks and Voids, Appl. Phys. Lett. 79, 3071 (2001).

[63] V.I. Levitas, A.V. Idesman, and E. Stein, Finite Element Simulation of Martensitic Phase Transitions in Elastoplastic Materials, Int. J. Solids and Structures 35, 855 (1998).

[64] V.I. Levitas, Structural Changes without Stable Intermediate State in Inelastic Material. Part II. Applications to Displacive and Diffusional-Displacive Phase Transformations, Strain-Induced Chemical Reactions and Ductile Fracture, Int. J. Plasticity, 16, 851 (2000).

[65] A.V. Idesman, V.I. Levitas, and E. Stein, Structural Changes in Elastoplastic Materials: a Unified Finite Element Approach for Phase Transformation, Twinning and Fracture, Int. J. Plasticity 16, 893 (2000).

[66] V.I. Levitas and M. Javanbakht, Advanced Phase Field Approach to Dislocation Evolution, Phys. Rev. B 86, 140101 (2012).

[67] V.I. Levitas and M. Javanbakht, Phase Field Approach to Interaction of Phase Transformation and Dislocation Evolution. Appl. Phys. Lett. 102, 251904 (2013).

[68] V.I. Levitas and M. Javanbakht, Phase Transformations in Nanograin Materials Under High Pressure and Plastic Shear: Nanoscale Mechanisms, Nanoscale 6, 162 (2014).

[69] A.A. Boulbitch and P. Toledano, Phase Nucleation of Elastic Defects in Crystals Undergoing a Phase Transition, Phys. Rev. Lett. 81, 838 (1998).

[70] A.A. Boulbitch and A.L. Korzhenevskii, Self-Oscillating Regime of Crack Propagation Induced by a Local Phase Transition at its Tip, Phys. Rev. Lett. 107, 085505 (2011).

[71] V. I. Levitas and M. Javanbakht, Interaction between phase transformations and dislocations at the nanoscale. Part 1. General phase field approach. J. Mech. Phys. Solids, 82, 287-319 (2015).

[72] M. Javanbakht, V. I. Levitas, Interaction between phase transformations and dislocations at the nanoscale. Part 2. Phase field simulation examples. J. Mech. Phys. Solids, 82 (2015) 164-185.

[73] V.I. Levitas and A.M. Roy. Multiphase phase field theory for temperature- and stress-induced phase transformations. Phys. Rev. B, 91, 174109 (2015).

[74] R. Lipowsky, Critical Surface Phenomena at First-Order Bulk Transitions, Phys. Rev. Lett. 49, 1575 (1982).

[75] V.I. Levitas and K. Samani, Melting and Solidification of Nanoparticles: Scale Effects, Thermally Activated Surface Nucleation, and Bistable States, Phys. Rev. B 89, 075427 (2014).

[76] V.I. Levitas, Z. Ren, Y. Zeng, Z. Zhang, and G. Han, Crystal-Crystal Phase Transformation via Surface-Induced Virtual Pre-Melting. Phys. Rev. B 85, 220104 (2012).

[77] A.E. Lobkovsky and J.A. Warren, Phase Field Model of Premelting of Grain Boundaries, Physica D 164, 202 (2002).

[78] V.I. Levitas, Crystal-Amorphous and Crystal-Crystal Phase Transformations via Virtual Melting, Phys. Rev. Lett. 95, 075701 (2005).

[79] J. Luo and Y.M. Chiang, Wetting and Prewetting on Ceramic Surfaces, Ann. Rev. Mater. Res. 38, 227 (2008).

[80] V.I. Levitas and K. Momeni, Solid-Solid Transformations via Nanoscale Intermediate Interfacial Phase: Multiple Structures, Scale, and Mechanics Effects, Acta Mater. 65, 125 (2014).

[81] K. Momeni and V.I. Levitas, Propagating Phase Interface with Intermediate Interfacial Phase:

Phase Field Approach, Phys. Rev. B 89, 184102 (2015).

[82] V.I. Levitas and I.B. Ozsoy, Micromechanical Modeling of Stress-Induced Phase Transformations. Part 1. Thermodynamics and Kinetics of Coupled Interface Propagation and Reorientation, Int. J. Plasticity 25, 239 (2009).

[83] V.I. Levitas and I.B. Ozsoy, Micromechanical Modeling of Stress-Induced Phase Transformations. Part 2. Computational Algorithms and Examples, Int. J. Plasticity 25, 546 (2009).